Snowman-shaped particles at the oil-water interface

Bachelor thesis

Rutger Kok
July 13, 2016

Supervisors: Fuqiang Chang and Willem Kegel
Van 't Hoff Laboratory for Physical and Colloid Chemistry
Debye Institute for Nanomaterials Science

Utrecht University

Abstract

Snowman-shaped polystyrene-based particles of about 2 μm in size were synthesized. The lobes are chemically different; the seed lobe can be modified without affecting the protrusion lobe, as confirmed fluorescence microscopy. For the interface assembly, the particles were spread on a decane-water interface. Here, we used optical microscopy to observe the structures that were formed by the particles, caused by shape-induced capillary attractions. We do see promising dimer structures, although there are always many aggregates present. The aggregates keep growing over time. The particles are not yet very homogenous in size, nor in shape. This is probably one of the reasons why the structures that were formed at the interface do not have much ordering yet.

Table of Contents

1 Introduction

Self-assembly is the spontaneous process of formation of ordered structures starting from a disordered structure. [1] Self-assembly processes are ubiquitous in nature; the formation of virus capsids, the folding of proteins and the formation of cell membranes are all examples of self-assembly. [1]

In molecular self-assembly, molecules are used as the primary building blocks. However, it is often convenient to use colloidal particles instead. Just like molecules, colloids can move spontaneously, can interact with each other and can be dispersed in liquids. [2]

For colloid science and engineering, it is crucial to understand the interaction forces between colloids. [3]. In the past, we have seen extensive research on colloidal hard spheres. The forces between anisotropic particles are less well-understood. [4]

The interface between oil and water offers an interesting opportunity for research. [3] Particles are easily trapped at this interface [5], creating what is essentially a two dimensional world. In this world, there are only two forces that play a significant role: the attractive capillary interactions and the repulsive electrostatic interactions. [3]

We can tune these forces by changing the properties of the particles at the interface. This could allow us to use self-assembly to create ordered structures. [6] Formed structures can be used for organic synthesis, separation techniques and as support for catalysts. [7] The structures may also be used as basic building blocks for hierarchical self-assembly. [8]

The goal of this project is to synthesize uniform-sized, smooth, snowman-shaped colloids based on polystyrene. The particles must be stable at a decane-water interface, without requiring surfactants. We hope that the particles will form ordered structures at this interface.

The particles are about 2 μm in size and consist of two lobes: a spherical seed and a protrusion. See Figure 1. The seed of the particle is a core-shell particle: the core of the seed lobe is made of polystyrene, while the shell also contains silane groups. The protrusion lobe contains no silane groups, making the surface of seed and the protrusion chemically different. This means that we are creating so-called Janus particles. [9]

It is possible to use the silane groups to modify the seed lobe, without modifying the protrusion lobe. We will make use of this to selectively make the seed lobe fluorescent in one experiment, and hydrophobic in another experiment.

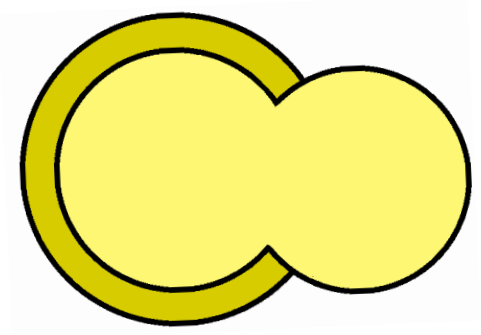

Figure 1 – drawing of snowman-shaped particle. The lobe on the left is called the seed lobe, the lobe on the right is called the protrusion lobe.

2 Theory

Micrometer-sized particles prefer a spherical shape more strongly than larger particles. The reason for this is as follows. For smaller particles, a larger percentage of atoms resides at the surface, so the surface tension is relatively high. In order to minimize the surface energy, particles must adopt a spherical shape.

For this reason, uniform anisotropic nanoparticles are more difficult to synthesize than spherical particles. Nevertheless, a wide variety of methods to prepare anisotropic nanoparticles have been developed. [10]

2.1 The synthesis

In this paper a method called seeded suspension polymerization is used. The synthesis is based on a method developed by Park et al. [10] Park and coworkers were able to synthesize particles with varying protrusion sizes. Their core-shell particles consisted of a core of linear polystyrene and a shell of a polymer made using styrene and 3-(Trimethoxysilyl)propyl acrylate (TMSPA). Their protrusions consisted of a copolymer made using styrene and sodium p-styrenesulfonate (NaSS).

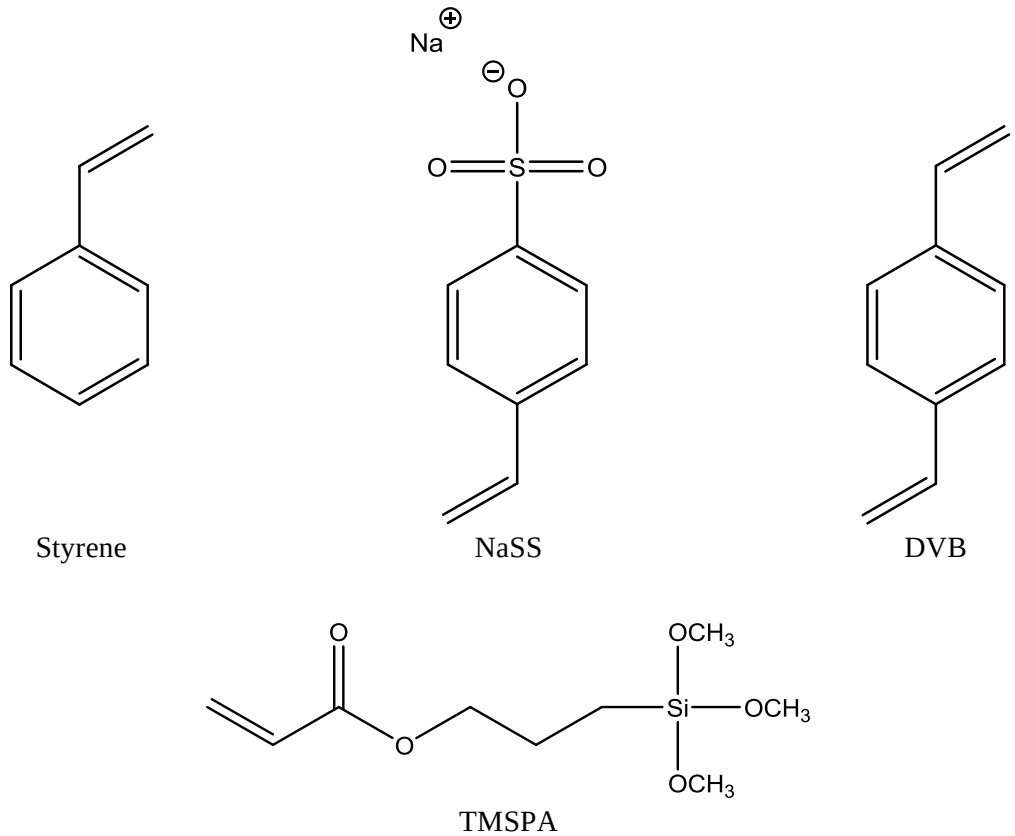

Styrene NaSS DVB

TMSPA

Figure 2 – monomers and comonomers. Styrene is the monomer, all the others are comonomers. NaSS is a salt, DVB a crosslinker and TMSPA provides functional groups.

We follow the same approach. One difference is that we will also use toluene to swell the core-shell particles. Another difference is that for some of our experiments, we will create a more crosslinked core-shell particle by adding divinylbenzene (DVB) as a comonomer.

The core-shell particles can be made by adding TMSPA, azobisisobutyronitrile (AIBN, an initiator), styrene and optionally DVB to linear polystyrene particles in water. The polystyrene particles will immediately start taking up the monomers (TMSPA, styrene and DVB), as if they were a sponge taking up water. This process is called swelling. The swelling must be done on a roller table, so that the hydrophobic styrene is mixed thoroughly with water.

The monomers can easily flow out of the linear polystyrene particles. This is called a phase separation, as the liquid monomer separates itself from the solid polymer. The hydrophobic monomer cannot diffuse into water, so the monomer has to stay on the particle. As the monomer can easily wet the hydrophobic linear polystyrene, a shell is formed around the particle. Because AIBN is present in the reaction mixture, this shell can be polymerized simply by heating. We now have particles with a core of linear polystyrene and a shell of a crosslinked polymer network.

These core-shell particles are used as seed particles for the next step. See Figure 3. In this step, the particles are swelled by a monomer, styrene in this case. Styrene causes the polystyrene network to be stretched. The linear core of the particles can expand indefinitely, but the crosslinked shell cannot. The swelling will therefore cause elastic stress on the shell of the particles.

Due to this stress, the monomer will phase separate from the particle. Unlike for some other syntheses [11] heating the particle is not required [10]. To phase separate, the monomer has to squeeze past the silane groups in the shell. When this happens, a droplet (also called a liquid protrusion) on the core-shell particle is formed. The formation of another shell instead of a droplet is practically impossbile, as the hydrophobic styrene will not wet the hydrophilic shell of the particle.

Later on, a polymerization reaction is used to solidify the droplet. From then on, the droplet is called a protrusion and is part of the particle.

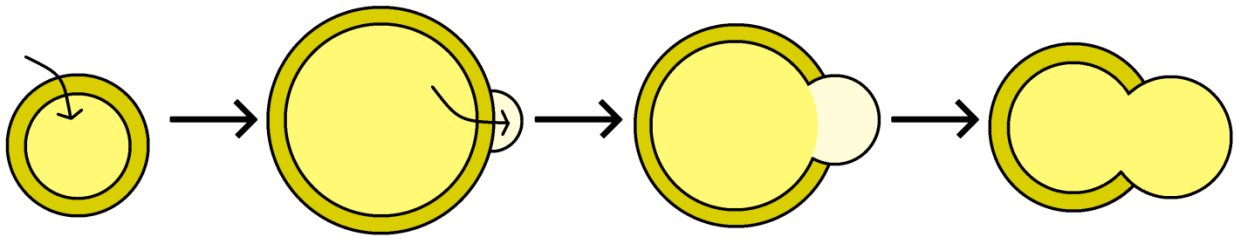

Figure 3 - mechanism of seeded suspension polymerization, starting at the core-shell particles. First, the core-shell particle is swollen, causing elastic stress. This stress is relieved when heating: some monomer leaves the particle and forms a droplet. This droplet is then polymerized into a solid protrusion.

When polymerizing, the protrusion lobe grows. The monomers required for this growth must come from somewhere. Apparently, there are remaining monomers in the seed lobe, which are transported to the protrusion during the polymerization reaction. [10]

2.2 Forces between particles at an oil-water interface

One of the goals of this project is to create ordered structures at the interface between decane and water. Trapping the particles at this interface is not a problem; the particles can be trapped easily at the interface. This is because particles at an interface reduce the area of this interface, which is very favorable for the high-energy decane-water interface. The particles essentially function in a similar way as surfactants. [5]

If the particles are very hydrophobic, a large part of the surface of the particles will be in oil. This means that they will have a high contact angle θ, see Figure 5. It is known that for spherical silica particles a well-ordered two-dimensional crystal structure can be formed if the contact angle of the particles is at least 129°. [12] On the other hand, less hydrophobic particles (with a smaller contact angle) form disordered structures and aggregate. [12] See Figure 4.

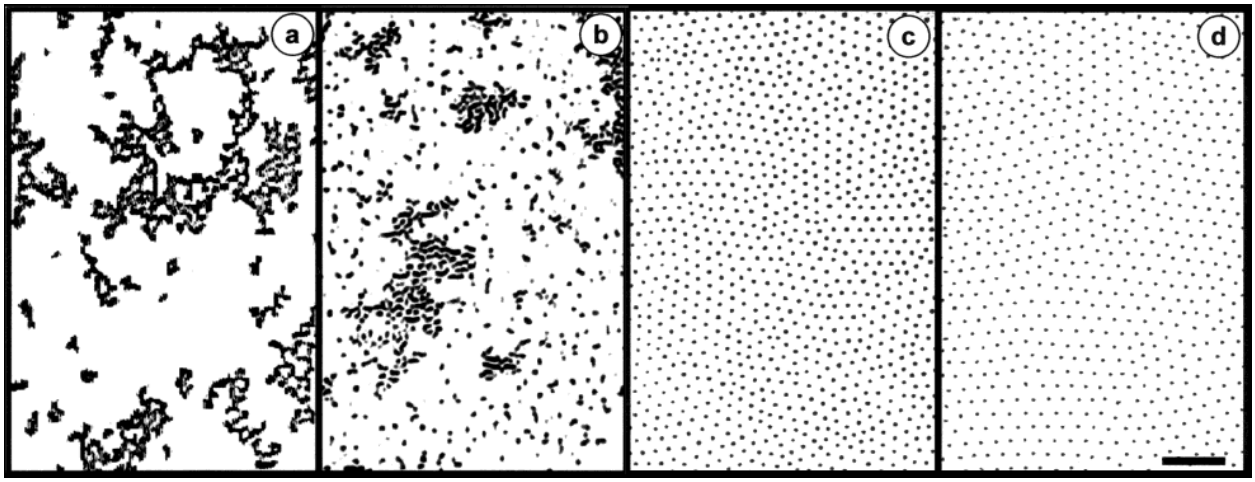

Figure 4 - Monolayers of silica particles, diameter 1 μm, with contact angles of (a) 70°, (b) 115°, (c) 129°, and (d) 150° at the octane-water interface. We can see that a stable structure is formed when the contact angle is at least 129°. The scale bar represents 25 μm. This figure is reprinted from Figure 1 in [12].

To understand this better, we need to take a look at the several forces that affect the particles. Just like for particles in bulk, there are repulsive and attractive forces. Yet, at interfaces the forces are more complex than in bulk. [13]

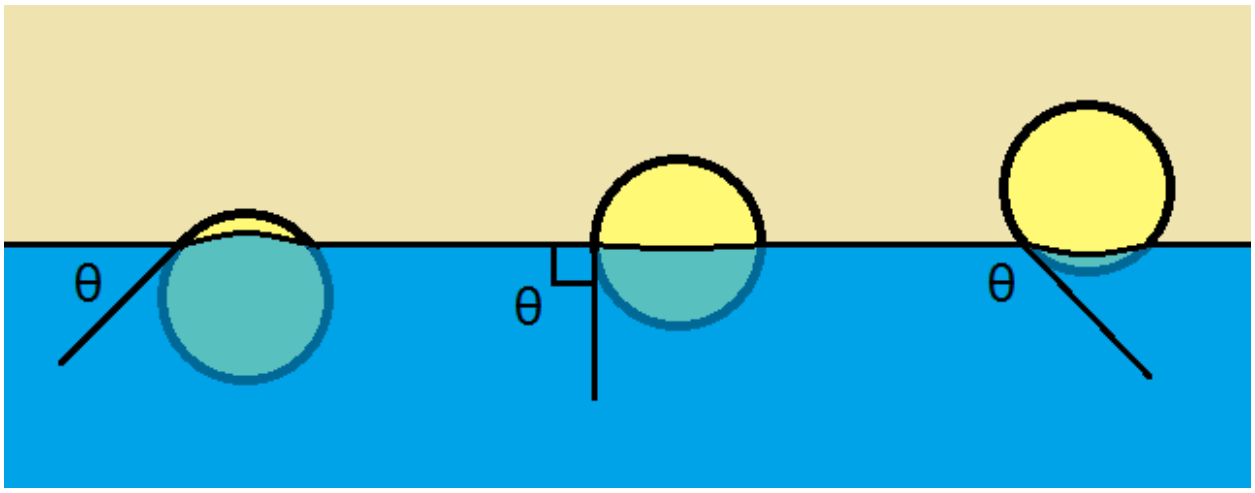

Figure 5 – from left to right: increasingly hydrophobic particles with a uniform surface at an oil (yellow) – water (blue) interface. The particles do not deform the interface, so the interface is completely flat.

For charged, spherical particles, the repulsive force is the dipole-dipole- interaction force, which makes $F_{repulsive} \propto r^{-4}$, where r is the distance between the particle centers. [3] This interaction can occur through both water and oil, so we have two different dielectric constants. This greatly enhances this force at the interface, compared to a bulk system. [14] Unfortunately, because of the two dielectric constants calculating the force is more complex. [13]

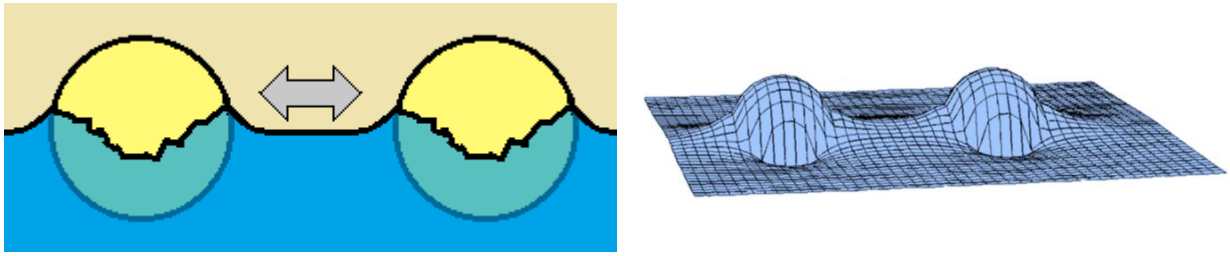

Figure 6 – left: chemically heterogeneous particle at an oil-water. The interface is deformed, which causes capillary attractions between the particles. Right: 3D-view of the deformation of the interface of these particles. The right image is based on Figure 2 of [15].

The attractive force is the capillary force. [3] This force arises from a deformed interface, induced by particles. [3] The deformed interface causes an excess interface area, which can be minimized when the particles change their position and orientation. [15] When two particles have menisci of the same sign (so both menisci are pointing upwards or both menisci are pointing downwards) the particles will attract. [15]

What about the van der Waals force? Reynaert et al. claim that "for micrometer-sized particles at oil-water interfaces, the van der Waals interaction is significant and will act at a distance corresponding to the order of the particle radius for polymeric particles at the oil-water interface" [16]. However, at an interface, distances between particles are typically much larger than the particle radius, so the van der Waals force is negligible. [3] [16]

Together, this allows us to express the total force on a particle as $F_{total} = F_{repulsive} + F_{capillary}$. [3]

2.3 The capillary force

As the capillary force arises from a deformed interface, we can conclude that there will be no capillary attractions if particles do no deform the interface at all. And indeed, smooth, chemically homogenous, spherical particles will not attract each other. [3] See Figure 5. On the macroscale, gravity is usually the cause of interface deformation. [3] However, for micrometer-sized particles, the gravitational force is not strong enough to cause attraction between the particles. [3]

For our particles, there are three causes of the deformed interface. Surface roughness, chemical heterogeneity and the anisotropic shape of our particles all play a role. [16]

Surface roughness can explain why capillary attractions exist even when using spherical and chemically homogenous particles. [3] In this case, the capillary force scales as $F_{capillary} \propto -r^{-5}$. As we will see during our experiments, particles with a rough surface will quickly aggregate at the decane-water interface.

Chemical heterogeneity also causes capillary attractions. For example, consider a particle that is hydrophobic on one side, and hydrophilic on the other side. Between both sides, there is a transition area. This forces excess oil-water interface to be created, which can be reduced if the particles come into contact.

Finally, the shape of the particles plays an important role. [3] [4] [17] Spherical particles can only be moved to find an energy minimum, but nonspherical particles can also be rotated. When this happens, the contact line of the interface is not flat anymore. For polystyrene-based particles, several people have measured the capillary interactions at an oil-water interface. Loudet et al. [17] observed aggregation upon contact for ellipsoidal particles; the particles aligned tip-to-tip, and particles with a

silica shell aligned side-to-side. They found out that $F_{capillary}$ scales with $-r^{-5}$ to $-r^{-4}$, depending on the orientation of the ellipsoids. [17] Park et al. found out that $F_{capillary}$ scales with $-r^{-6.8}$ to $-r^{-5}$ for cylindrical particles [4] and with $-r^{-5}$ for dumbbell-shaped particles. [3]

2.4 Formation of structures at the oil-water interface

Armed with this knowledge, we can speculate about the structures that can be formed at the decane-water interface. We will see that all three interactions that were mentioned above will play a role. However, in the following discussion we will assume that the only attractive force is the shape-induced capillary force. We will also assume that there is some repulsive force between the particles.

Excluding the other interaction forces seems like an oversimplification, and it most likely is. Our particles are Janus particles, so there is a certain amount of chemical heterogeneity. Futhermore, the surface of the particles will not be completely flat. However, this simple model allows us to do some predictions. Later on, we will talk about the effects of the other interactions.

What structures will then be formed? If we assume that all particles are initially at the interface as monomers, the first step towards the formation of a structure will be the formation of dimers. Shape-induced capillary attractions are caused by deviations from the spherical shape, so we will assume that these attractions are the strongest at the point where the two lobes of a particle come into contact (Figure 7, left). This causes a quadrupole-like interaction (Figure 7, right).

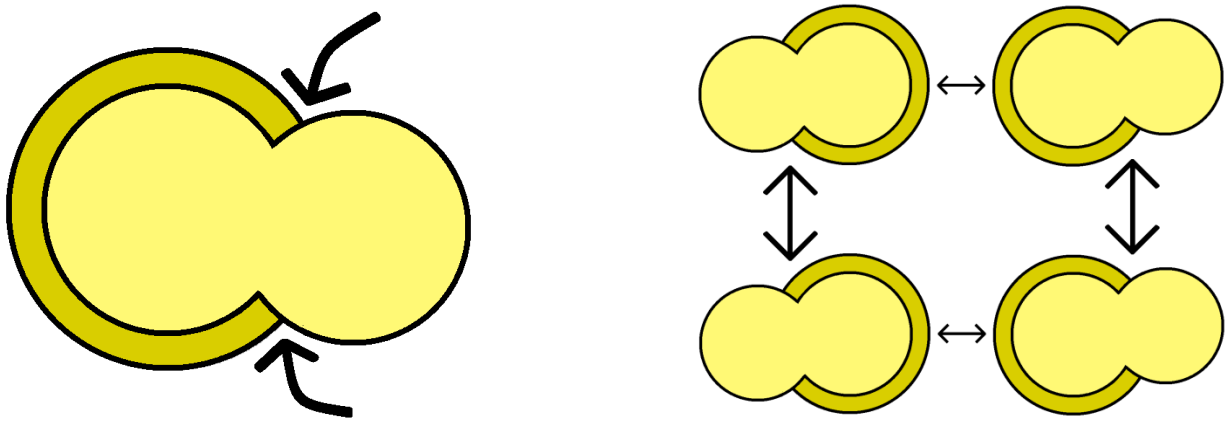

Figure 7 – left: the locations (marked by arrows) where the shape-induced capillary attraction is the largest. Right: this causes an interesting effect where the particles interact like quadrupoles.

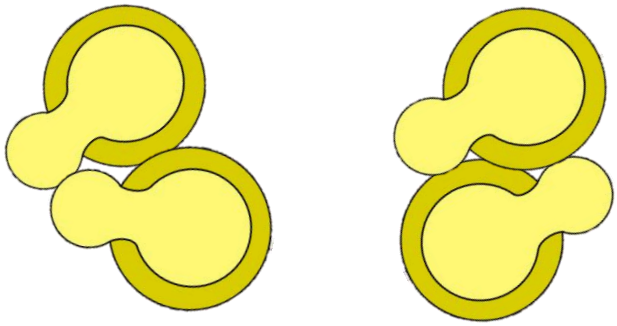

Figure 8 – two possible dimer structures. The left structure is called the cis structure, while the right structure is called the trans structure.

Based on this model, there are two possible configuration that can occur when two particles come into contact: a cis structure where the protrusions are on the same side (Figure 8, left) and a trans structure where the protrusions are on different sides (Figure 8, right).

These aggregates can grow further. If all particles would attach in the cis conformation, a ring-like structure will be formed (Figure 9, left). If all particles would attach in the trans conformation, a line-like structure would be formed (Figure 9, right).

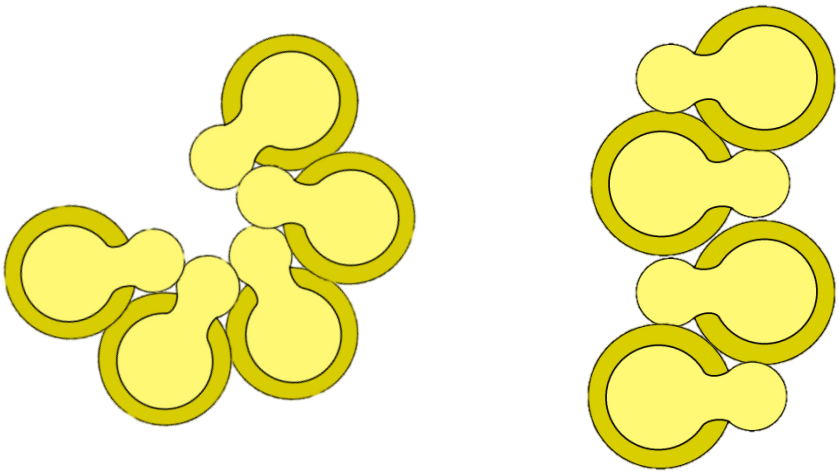

Figure 9 – formation of larger structures when either only cis attachment is used (left) or only trans attachment is used (right).

A combination of cis and trans attachments is also possible, in this case the structures will be more chaotic.

The biggest assumption that we have made here is that the only attractive force is the shape-induced capillary attraction force. Our particles are Janus particles, so this assumption will not hold. The chemical heterogeneity and hydrophobicity of the particles will cause them to be pinned in a certain orientation. We will modify our particles to reduce the chemical heterogeneity, and increase the overall hydrophobicity.

Especially in our earlier experiments, the surface of our particles will be very rough, which causes additional capillary attractions. We will try to reduce the surface roughness to reduce these attractions.

Even if we synthesize ideal particles, it is still possible for the above model to be incorrect. The reason for this is that we cannot assume that the particles will always form structures with the lowest energy. There will be a certain amount of kinetic control when the particles are spread on the interface.

3 Experimental

Throughout all experiments, all water that was used in samples was purified using a Milli-Q water purification system. All decane (Sigma-Aldrich, ≥ 99%) was purified prior to use: polar components were removed from decane using adsorption onto aluminum oxide particles. [16] All other chemicals were used as received.

For all optical microscopy images (both of particles in bulk and of particles at the interface), an unmotorized Nikon Inverted Microscope, Eclipse Ti-U was used with an Infinity x32c 180850 camera.

3.1 Preparation of linear polystyrene particles

90 mg AIBN (Argos Organics) was added to a flask, after which a mixture of 8 mL styrene (Sigma-Aldrich) and 40 mL methanol was added to this flask. A solution of 10 mL H_2O with 130 mg NaSS (Aldrich) was then added to the flask. While stirring, the flask was degassed with N_2 for 30 minutes. After that, the polymerization was started by placing the flask in an oil bath for 30 minutes, while stirring continued. After that time, a mixture of 2 mL styrene and 10 mL methanol was added, and polymerization continued for another 20 hours.

The sample was washed with water: some water was added to the flask, the supernatant (which now contains the sample) was centrifuged for 30 minutes at 2000 rpm (931 g). The solid remainder was discarded. The centrifuged sample was decanted and then this washing procedure was repeated two more times.

The solid contents were measured by letting a bit of the sample (for example 100 μL) dry on a plate under a heating lamp.

3.2 Preparation of core-shell particles

Three samples were prepared of core-shell particles. All samples contain polystyrene spheres, AIBN, water, styrene and one or more comonomers. Which comonomers were used depends on the sample. Initially, core-shell particles containing TMSPA (Alfa Aesar, 94%) and DVB (Aldrich, 55%, mixture of isomers, tech. grade) were used, but later on particles without DVB were synthesized. The exact amounts can be found in Table 1. The samples were prepared in glass vials with a Teflon cap.

The mass ratio between the added monomers styrene and TMSPA and the polymer polystyrene is called the swelling ratio. In other words: adding more monomer will result in a higher swelling ratio.

Table 1 – preparation of core-shell particles from linear polystyrene particles

CPS-TMSPA	**LPS-TMSPA-1**	**LPS-TMSPA-½**	**Explanation**
37.1 μL TMSPA	62.2 μL TMSPA	31.1 μL TMSPA	Comonomer, 11 vol% of TMSPA + styrene volume
16.9 μL of DVB	-	-	For crosslinking the polymer, 5 vol% of TMSPA + styrene volume
3.4 mg AIBN in 300 μL styrene	5.66 mg AIBN in 503 μL styrene	2.83 mg AIBN in 251.6 μL styrene	AIBN is the initiator, 1 g/mL monomer volume. Styrene is the monomer.
4 mL of H_2O	6 mL of H_2O	6 mL of H_2O	Purified using a Milli-Q system
1 mL of 307 mg/mL polystyrene	2 mL of 257 mg/mL polystyrene	2 mL of 257 mg/mL polystyrene	With this weight percentage and these amounts, the swelling ratio is exactly 1 for CPS-TMSPA and LPS-TMSPA-1, and exactly 0.5 for LPS-TMSPA-½

The samples were left swelling on a roller table (40 to 50 rpm). The samples with a swelling ratio of 1 were left for 20 hours on the roller table, while the sample with a swelling ratio of 0.5 was left for 10 hours on the roller table The samples were then placed in an oil bath, and were left rotating for about 24 hours at 70 rpm and 70 °C, so that the coating reaction was initiated.

The particles were then washed three times in water, centrifuging at 2000 rpm (931 g) for 20 minutes in each round.

3.3 Creating protrusions

One of the main goals of this project was to synthesize uniform, nonspherical particles. As different parameters were investigated, no two syntheses were the same. The general procedure is described below, while the exact amounts can be found in the results section.

As the required amounts of additives will always depend on the amount of monomers, it is convenient to define a "weight/volume percentage", or wt/vol%. 1 wt/vol% of *X* is defined as 0.01 g of *X* per 1 mL monomer.

A typical procedure is described below. A certain amount (0.5 mL to 2 mL, depending on the concentration) of the core-shell particles was mixed with a certain amount of NaSS (Aldrich) dissolved in water (1 mg/mL). Usually the amount of solid NaSS was 0.5 wt/vol%. A mixture of styrene and AIBN (always 1 wt/vol%) was added afterwards. The particles were swelled on a roller table for about 20 hours. After that, the reaction was initiated at 80 °C or 70 °C for about 7 hours in an oil bath, at an angle of 60°.

The particles based on CPS-TMSPA were then washed three times in water, while the particles based on LPS-TMSPA were washed three times with ethanol (Emsure, absolute for analysis). During each washing step, the particles were centrifuged at 2000 rpm (931 g) for 20 minutes.

3.4 Swelling ratio

In the synthesis of protrusions a lot of parameters can be varied. We have already seen the swelling ratio for the synthesis of core-shell particles; it was the mass ratio between the added monomers and the existing polymers. This exact definition can also be applied to the creation of the snowman-shaped particles.

Up to a certain limit, the more monomers are present, the more can be taken up by the particle, and the bigger the seed particle grows. This results in bigger protrusions. [18] However, the core-shell particles can only take up a finite amount of monomers; if the concentration of the monomers is too high, we will not see a further increase in protrusion size. [18] At very high concentrations, it is even possible for secondary nucleation to occur. [18]

3.5 Crosslinking density

Another parameter in the synthesis is the crosslinking density. This parameter represents the degree of crosslinking between monomers. As mentioned earlier, polystyrene normally forms linear polymers. To be able to generate elastic stress, we used DVB as a comonomer to crosslink the shell of the core-shell particles.

More crosslinking in the seed particles increases the elastic stress when swelling. This means that the monomer is more easily expelled, and the formed protrusions will be larger. However, this only works up to a certain limit. If the seeds are too crosslinked, less monomer can be taken up, and the protrusions

will be smaller. Another effect is that too much crosslinking leads to inhomogeneous networks. [18] The shell will become rough, which, as we will see, will make the particles less stable at the decane-water interface.

3.6 Toluene

To build up enough elastic stress for a protrusion to be formed, a certain minimum volume of monomer is required. [18] This means that there is also a certain minimum volume for the protrusions. As we just mentioned, we can decrease the minimum required volume by increasing the crosslinking density. For our desired particle shape, this method is not possible, as it would destabilize the particles too much.

Instead, we can reach the required volume by adding toluene. Just like styrene, toluene swells the particles and therefore generates elastic stress. Unlike styrene, it cannot be polymerized. When heating, the toluene will just evaporate.

In other words, adding toluene allows us to use smaller amounts of styrene than what would normally be possible.

It is important to note that we will include toluene in the weight/volume percentage as a monomer, even though technically it is not a monomer.

3.7 Interface experiment

In the so-called interface experiment, we look at particles at a decane-water interface using optical microscopy. Prior to injection, the sample containing the particles was washed five times with ethanol.

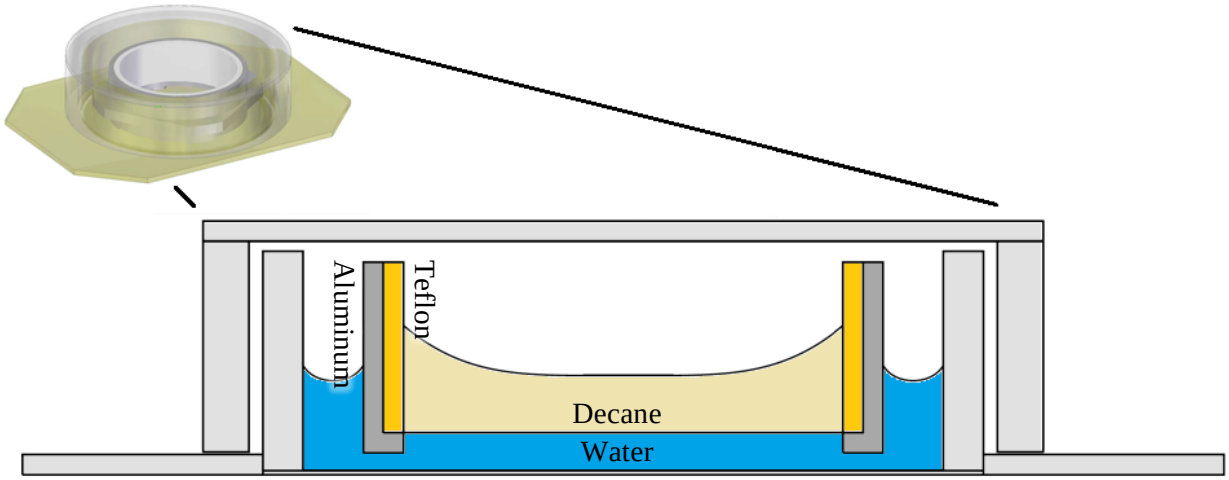

Figure 10 – the interface cell. The wall of the cylinder consists of two layers: an inner wall and an outer wall. There is space for water between the inner and the outer wall. There is also some space below the inner wall, so that water can flow. Decane puts pressure on water, so that most water is between the inner wall and the outer wall. The Teflon and aluminum sides keep the meniscus flat.

The cell that was used can be seen in Figure 10. It is designed to keep the meniscus flat. 1.8 mL of H_2O was added to the cell. The water then spreads across the whole bottom of the cell. 0.5 mL of purified decane was then added on top of the water layer. Note that the decane cannot flow beneath the inner wall, as decane will always sit on top of water.

The sample with the particles (1 to 2 µL, depending on the concentration) was injected into the water layer. The injection happens by moving a needle to the bottom of the vial, then moving the needle up a bit so that it no longer touches the bottom, and then injecting the particles slowly, but with a constant

speed, into the water layer. On the one hand, the needle may not touch the bottom of the vial, otherwise the particles would get stuck on the bottom of the vial. On the other hand, the needle must not be moved up too far, otherwise the particles may be injected into the decane layer, which causes aggregation.

0.2 mL of water then needs to be removed from the side to put the interface at the correct height for a flat interface. At this height, the contact angle is always pinned such that the decane will only touch Teflon and the water will only touch aluminum (see Figure 10). It is therefore very important to use exactly this amount of water.

3.8 Surface modification

Because hydrophilic particles on an oil-water interface tend to aggregate, the particles had to be made more hydrophobic. Normally, a certain percentage of the -OCH_3 groups of TMSPA are replaced by -OH under the influence of water. [19] To make the particles hydrophobic again, these -OH groups are replaced by -$OSi(CH_3)_3$ groups using hexamethyldisilazane. [20] See Figure 11.

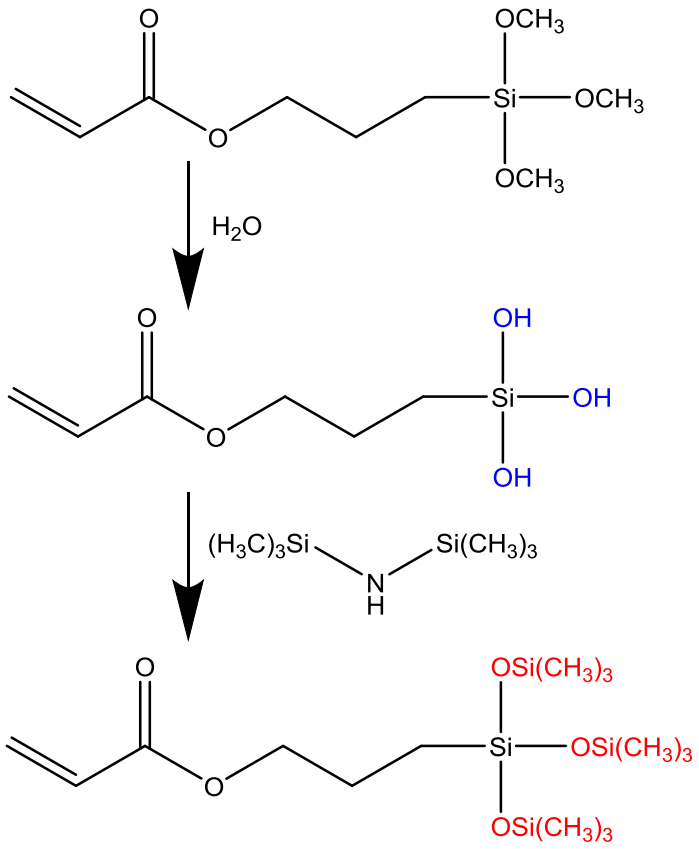

Figure 11 – surface modification reactions

The procedure for modification of the core-shell particles is as follows. A certain volume of the sample, such that the dry contents are 4 mg, is washed for ten times with ethanol. In the last round, exactly 1 mL of ethanol was added. 8 µL of hexamethyldisilazane (so 2 µL for each mg of particles) was added to this sample. Because this reaction is not catalyzed and therefore not very fast [20], the samples were left on a roller table for at least 48 hours.

3.9 Fluorescent labeling

Our particles should be chemically anisotropic. To check this, we use a dye (see Figure 12) that binds to the silane groups on our particles. If the silane groups are, as we expect, only on the shell of the seed lobe, we will see that only the seed becomes fluorescent. This proves that the particles are chemically anisotropic.

0.01428 mmol fluorescein isothiocyanate and 3.61 mmol APS were mixed with 10 mL of ethanol. This results in the formation of the dye molecule. The dye stock solution was stirred overnight in the dark and stored afterwards in a refrigerator (4 °C).

The rest of the procedure is mostly the same as for the surface modification: again 8 µL reactant (now the dye solution) was added to a washed solution containing 4 mg of particles. One difference is that the sample was washed only three times, and with water instead of ethanol.

The particles were viewed using a fluorescence microscope: a motorized Nikon Inverted Microscope, Eclipse Ti-E.

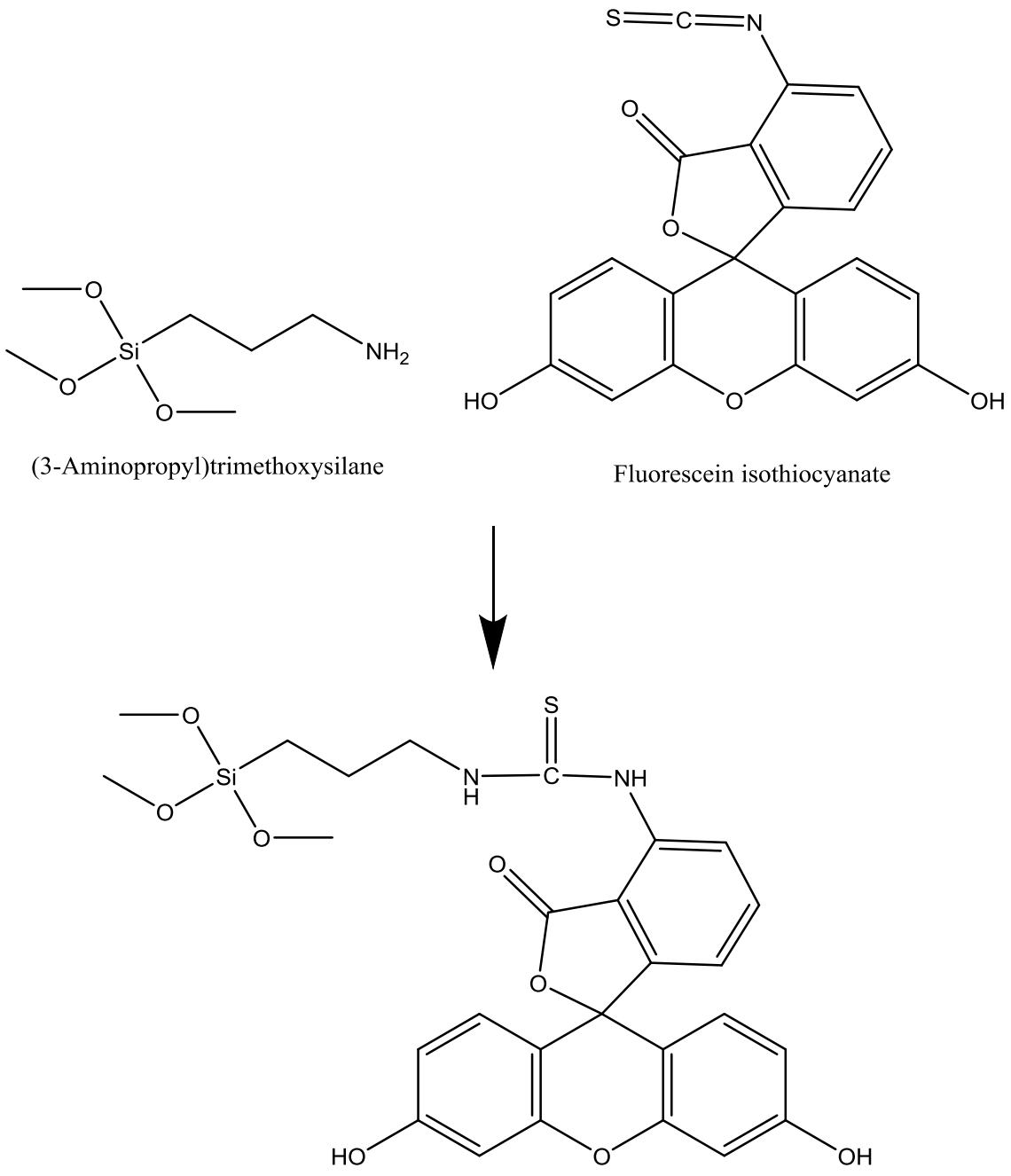

Figure 12 – creation of dye molecule using (3-aminopropyl)trimethoxysilane and fluorescein isothiocyanate

4 Results and discussion

4.1 Particles from crosslinked core-shell particles: synthesis and interface performance

Linear polystyrene (LPS) particles in water were prepared from styrene. The resulting suspension turned out to have a concentration of 307 mg/mL.

Using dynamic light scattering in water, the particle size was determined on a ZetaSizer Nano ZS. The size turned out to be 1.55 ± 0.13 μm.

The zeta potential was also measured on the same machine, but using laser Doppler micro-electrophoresis. The zeta potential was -65.1 ± 1.1 mV for particles in water and -34.8 ± 0.8 mV for particles in ethanol. This difference is quite large; it can probably be explained by differences in pH. For the synthesis experiments, we only used linear polystyrene in water, not in ethanol.

These LPS particles were used to create crosslinked core-shell particles. The LPS particles were swollen using styrene, TMSPA and DVB. The resulting crosslinked polystyrene core-shell particles are abbreviated as CPS-TMSPA particles.

To create protrusions, the CPS-TMSPA particles were swollen using styrene (swelling ratio = 3.74), 1 wt/vol% NaSS and 1 wt/vol% AIBN for 18 hours. After swelling, some protrusions were visible, but most particles were spherical, see Figure 13. There were also aggregates visible in the suspension. After polymerization (23 hours, 80 °C), the particles had formed large aggregates.

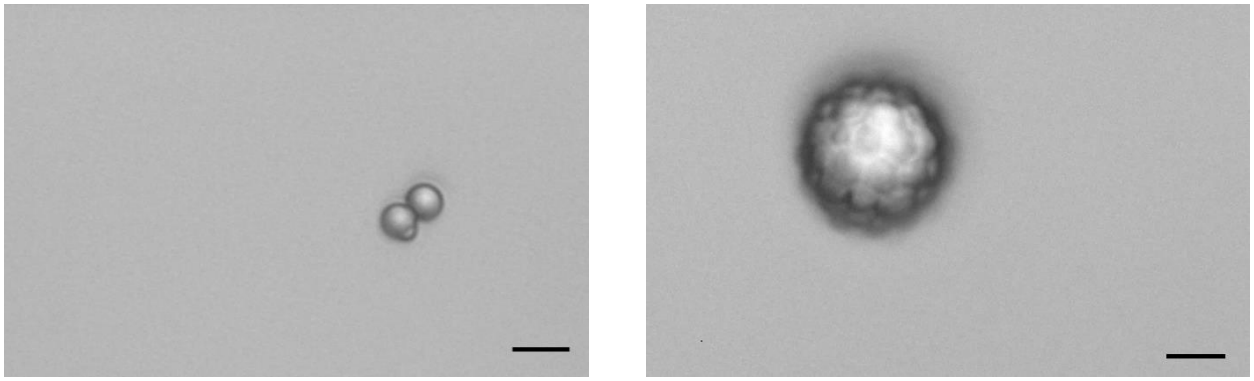

Figure 13 – optical microscopy images of the first protrusion experiment. In the sample, we could see both snowman-shaped particles and spherical particles. Frequently, these particles resided in aggregates. These images were taken using a 60x objective of the particles in water, just after swelling but before polymerization. Both scale bars are 5 μm.

We first lowered the NaSS concentration. NaSS was used to put a negative charge on the particle, which makes the particles stable in water. However, using a concentration that is too high causes the particles to aggregate. Later on, we also lowered the swelling ratio, which should reduce aggregation during the polymerization reaction. Together, this resulted in more optimized conditions: when mixing 0.5 wt/vol% NaSS, 1 wt/vol% AIBN and styrene (swelling ratio = 1.5), swelling for 17 hours and polymerizing for 6.5 hours, no more large aggregates were formed. Although a larger percentage of the particles had formed protrusions, there were still some spherical particles present. See Figure 14.

In none of the samples in this thesis we were able to get rid completely of the spheres, so from now on the presence of spherical particles along the snowman-shaped particles will not be mentioned anymore.

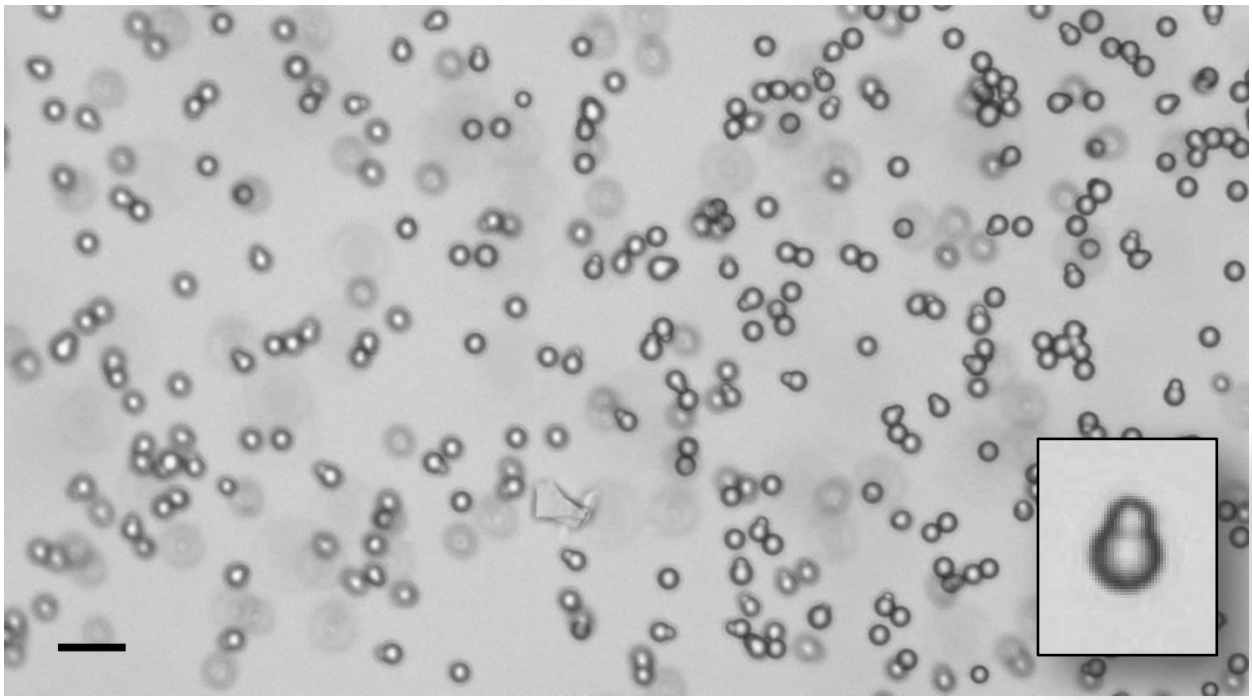

Figure 14 – particles created from CPS-TMSPA and styrene (swelling ratio = 1.5) in ethanol, 40x objective. The scale bar represents 10 μm. Inset: digitally zoomed in version of a particle visible in the larger photo.

At an oil-water interface, the particles were still not very stable. Although there are some trimers formed, most of the particles are in random aggregates. See Figure 15.

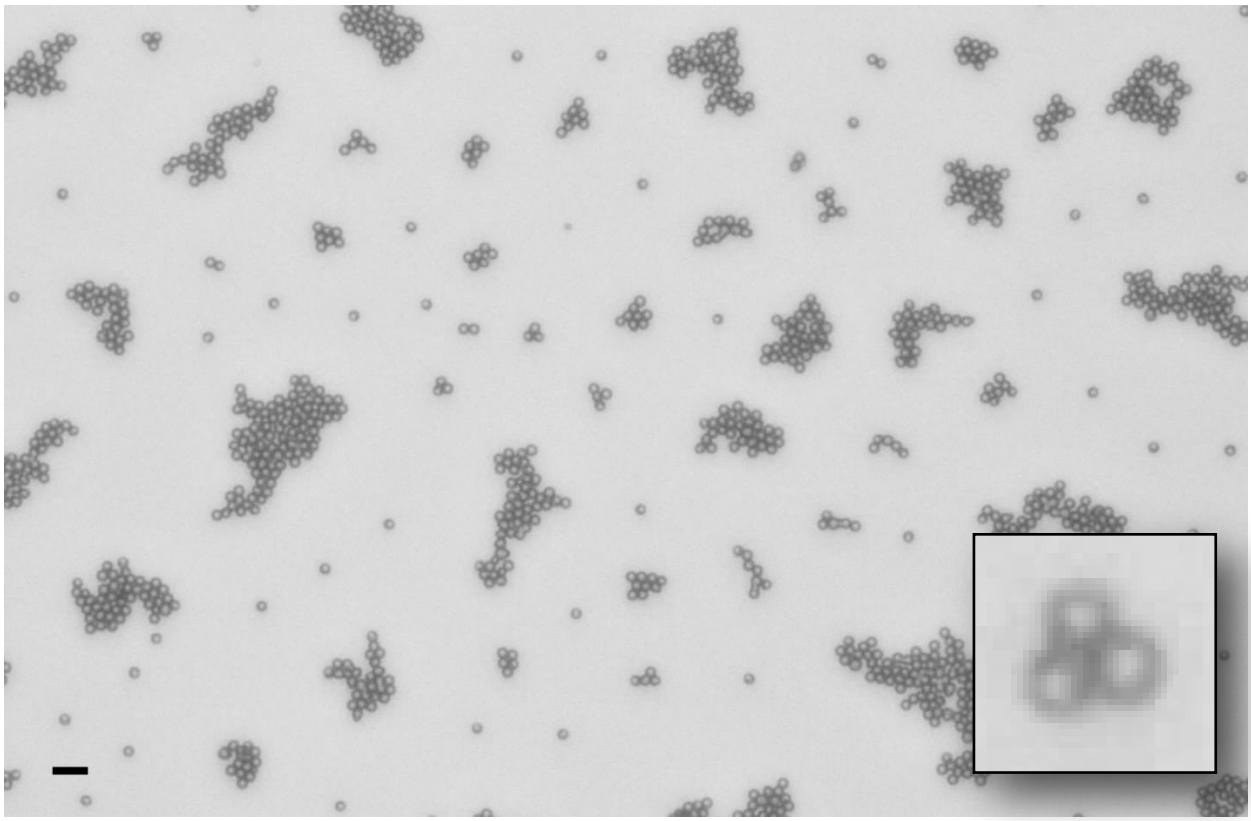

Figure 15 – the same particles as in Figure 14, now at the decane-water interface. Image taken using optical microscopy (20x objective).The scale bar represents 10 μm. Inset: a trimer, copied from the bigger image and zoomed in digitally.

In Figure 15, a trimer has been highlighted. The protrusions of this trimer structure are not visible, so it is unknown whether the protrusions are above, below or at the interface.

As chemical heterogeneity is one of the sources of capillary attractions, we have modified the particles to be more hydrophobic using hexamethyldisilazane (HMDS). This resulted in a more regular pattern at the oil-water interface, but there were still a lot of aggregates visible (Figure 16). Note how the seed lobes of the particles seem to attract each other.

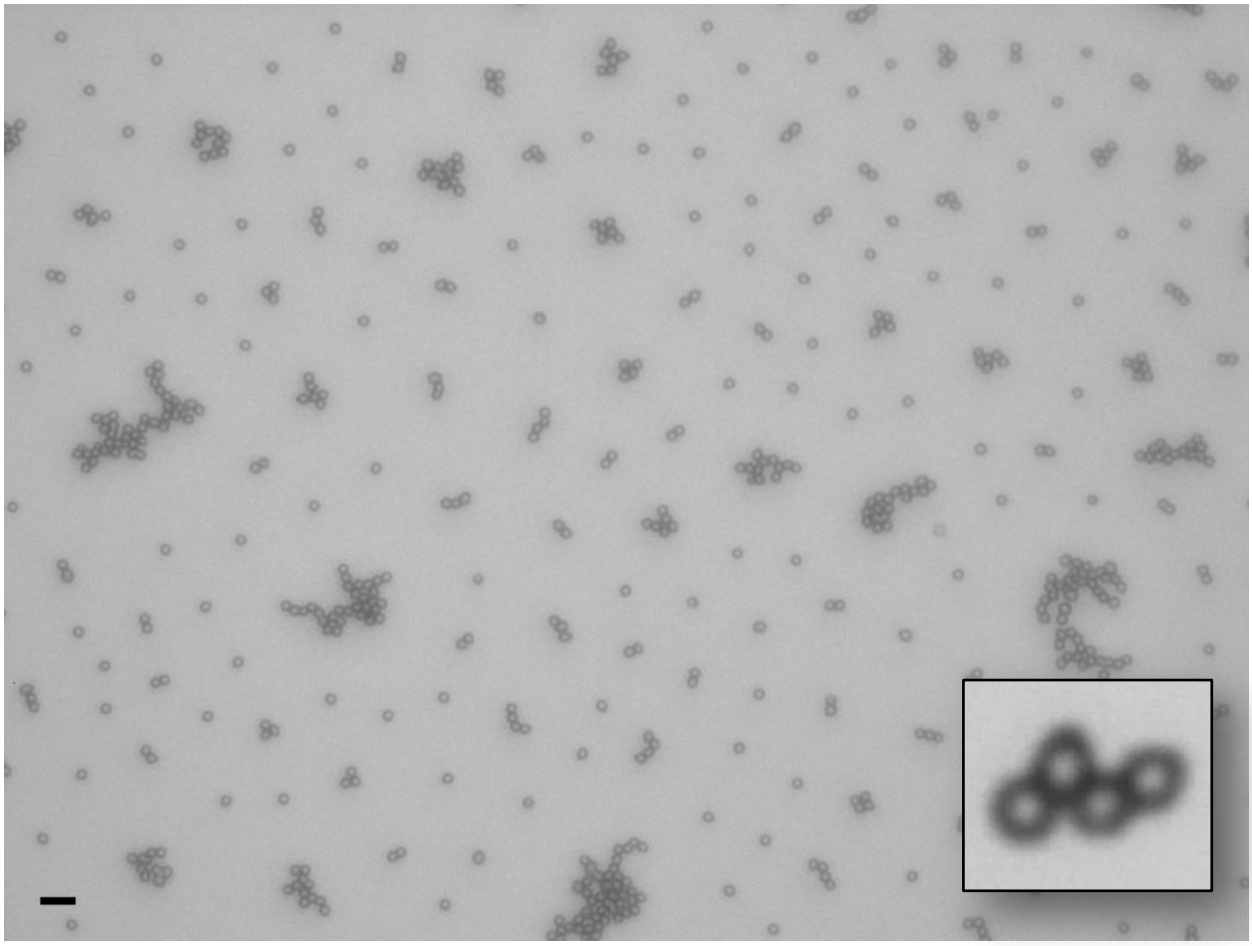

Figure 16 – particles at the decane-water interface. These particles are from the same batch as the particles used in Figure 14 and Figure 15, except that they are now modified using HMDS to make them more hydrophobic. The image was taken using optical microscopy; a 20x objective was used. The scale bar represents 10 μm. Inset: same particles, now viewed using a 40x objective. Note that the protrusion is at the exterior of the particle.

To tune protrusion size, a new synthesis was carried out where ⅓ of the styrene volume was replaced with toluene. The conditions now stated: 0.5 wt/vol% NaSS, 1 wt/vol% AIBN, styrene (swelling ratio = 1) and toluene (swelling ratio = 0.5), swelling for 18.5 hours and polymerizing for 5 hours. As noted on page 12, toluene can be used for swelling just like styrene, but unlike styrene it cannot be polymerized. This can be used to create smaller protrusions. In practice, not much difference was visible between the protrusions formed in previous experiment and the protrusions of this experiment: compare Figure 16 and Figure 17. Apparently, there is not much of a difference in size when changing the styrene swelling ratio from 1.5 to 1.

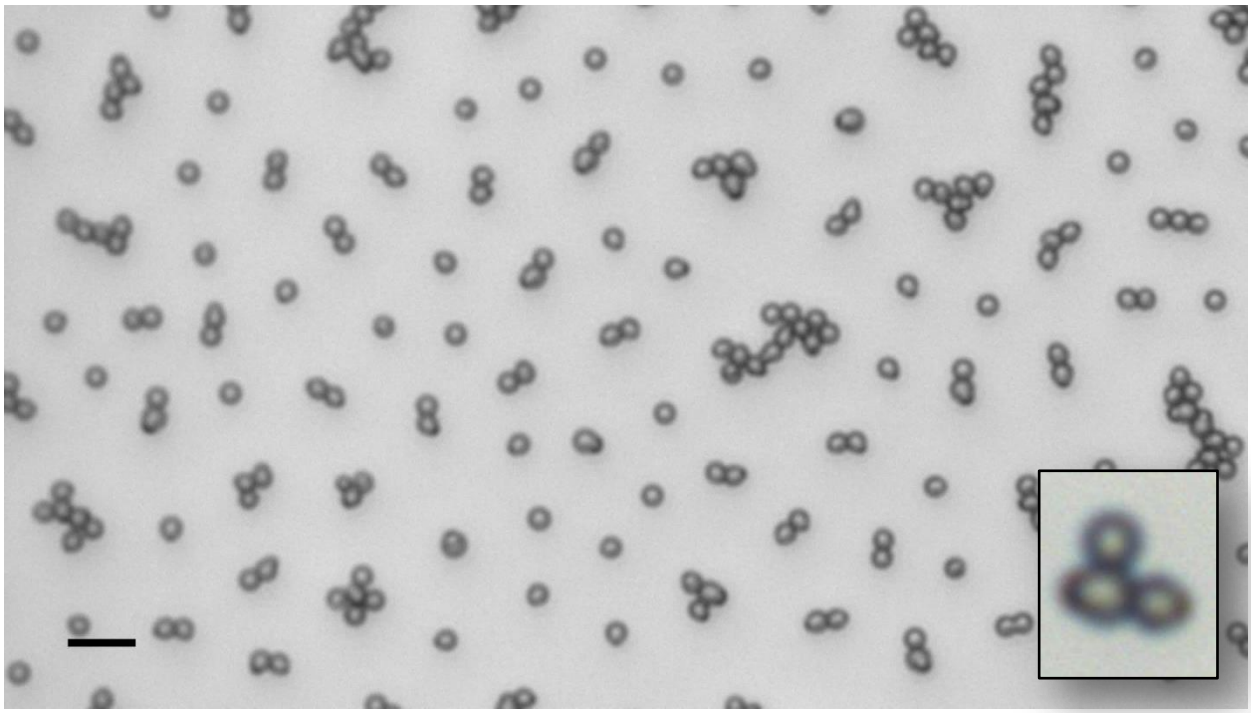

Figure 17 – particles at the decane-water interface. The particles were created using CPS-TMSPA, styrene (swelling ratio = 1) and toluene (swelling ratio = 0.5) and were modified using HMDS to be more hydrophobic. The image was taken using optical microscopy; a 40x objective was used. The scale bar represents 10 μm. Inset: part of the image, digitally zoomed.

To prove that these particles are indeed chemically anisotropic, a rhodamine-B isothiocyanate-based dye (Figure 12) was attached to the surface of the particles. In theory, the dye should absorb only on the TMSPA-containing shell of the seed particle, and not on the protrusion. In practice, some dye still absorbs physically to the protrusion, but we can see that more dye is absorbed on the seed particle. See Figure 18.

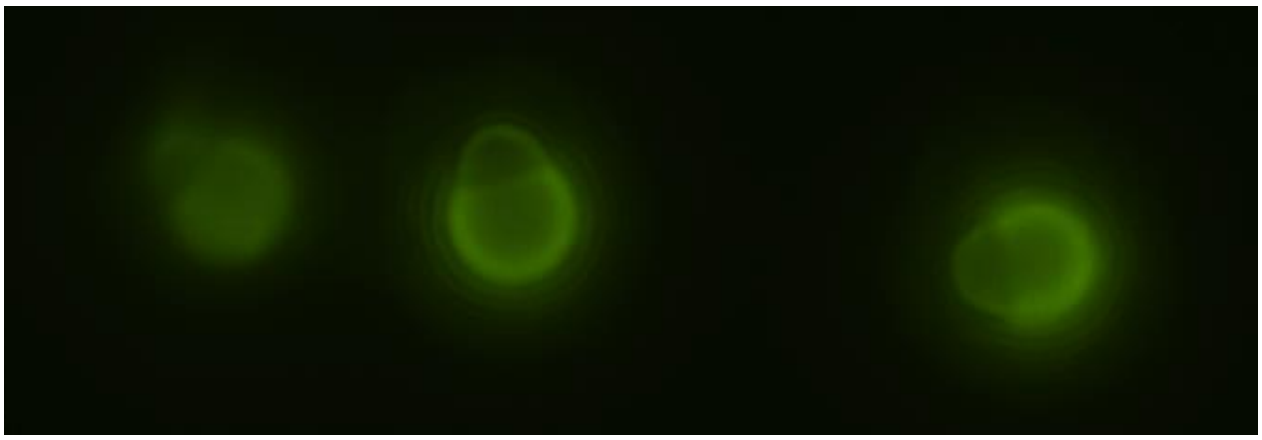

Figure 18 – image taken using fluorescence microscopy. We can see that the dye attaches more easily to the seed particle than the protrusion. The same particles as in Figure 17 were used, except that instead of modifying the particles with HMDS, the particles were modified using a dye (Figure 12) to be hydrophobic.

4.2 Particles from linear core-shell particles: synthesis and interface performance

In the previous section, we saw that the seed lobes tend to attract each other at the interface. The parts of the seeds that were touching each other were spherical, so shape-induced capillary attractions cannot be used to explains this. The seeds are also chemically homogenous, so only one possible cause for

capillary attractions remains: the surface roughness of the particles. To eliminate these undesired seed-to-seed attractions, we need to reduce the surface roughness of the particles.

To do this, core shell particles with no DVB were created. This does not mean that there is no crosslinking at all: TMSPA is also able to crosslink polystyrene chains. This is because TMSPA can be polymerized to itself by a condensation reaction [19] (Figure 19).

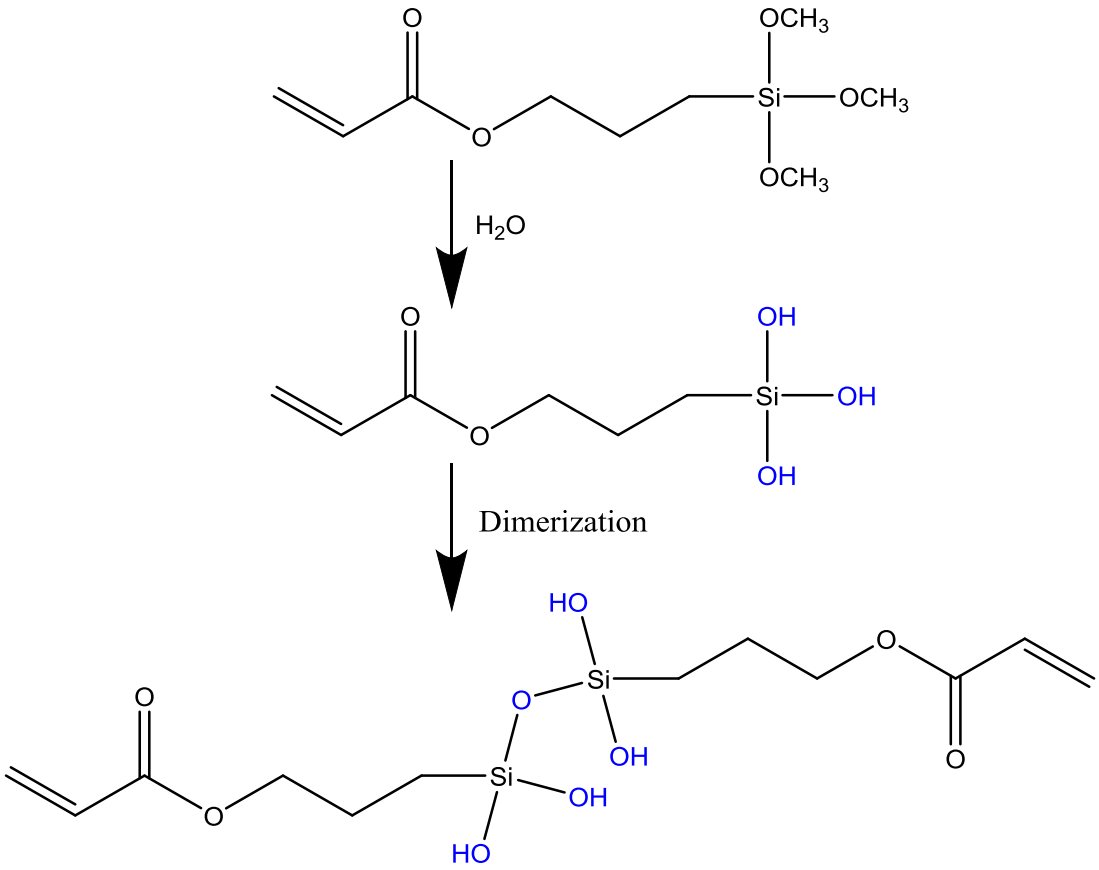

Figure 19 – dimerization of TMSPA in water. Note the double bonds at both ends of the structure; these can be used for crosslinking of polystyrene chains.

For creating the core-shell particles, a new batch of LPS particles were used. The LPS particles were viewed using TEM (Figure 20, left). By viewing 20 particles using TEM, it was determined that the particles have a diameter of 1.66 ± 0.06 μm.

Even though the shell of these particles is not completely linear, we will still call the particles linear polystyrene core-shell particles, abbreviated as LPS-TMSPA particles. The LPS-TMSPA particles were also viewed using TEM (Figure 20, right). Using 21 particles, it was determined that the particle diameter is 1.84 ± 0.16 μm.

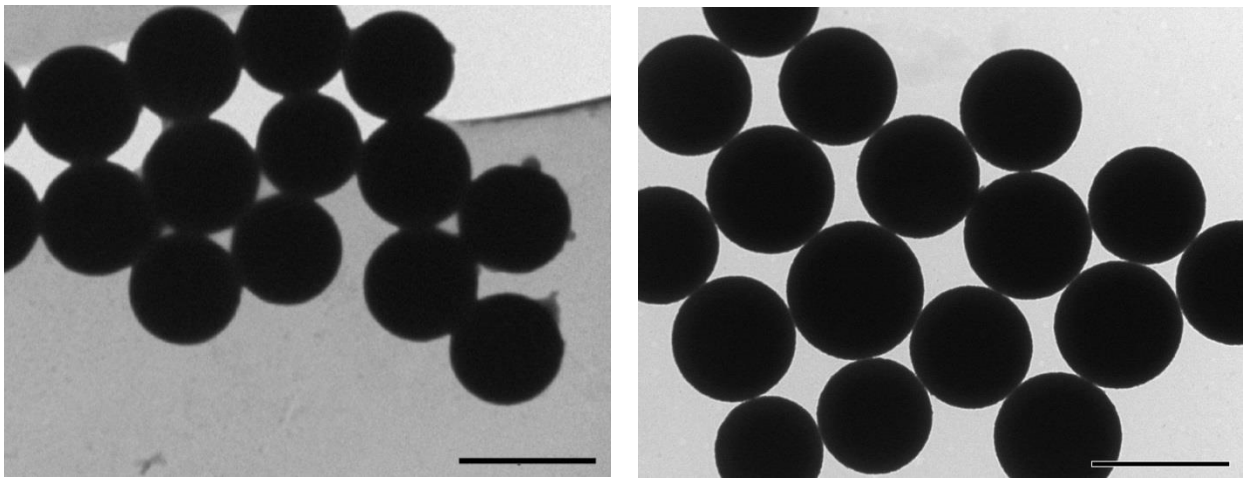

Figure 20 – left: TEM image of new batch of linear polystyrene particles. Right: TEM image of the core shell particles created from these particles. Both scale bars are 2 μm.

Using a less crosslinked particle has the unfortunate side effect that less elastic stress is generated, which makes growing a protrusion more difficult. [18] . Swelling ratios from 1.5 to 4 were tried, but we always saw aggregation during swelling.

Instead, an LPS-TMSPA with a lower swelling ratio (swelling ratio = 0.5) was prepared. This proved to be more successful: the shell of these particles is thinner than before, so less elastic stress is required. A swelling test with only toluene (swelling ratio = 4) yielded good results: the sample was stable in water and the particles formed protrusions.

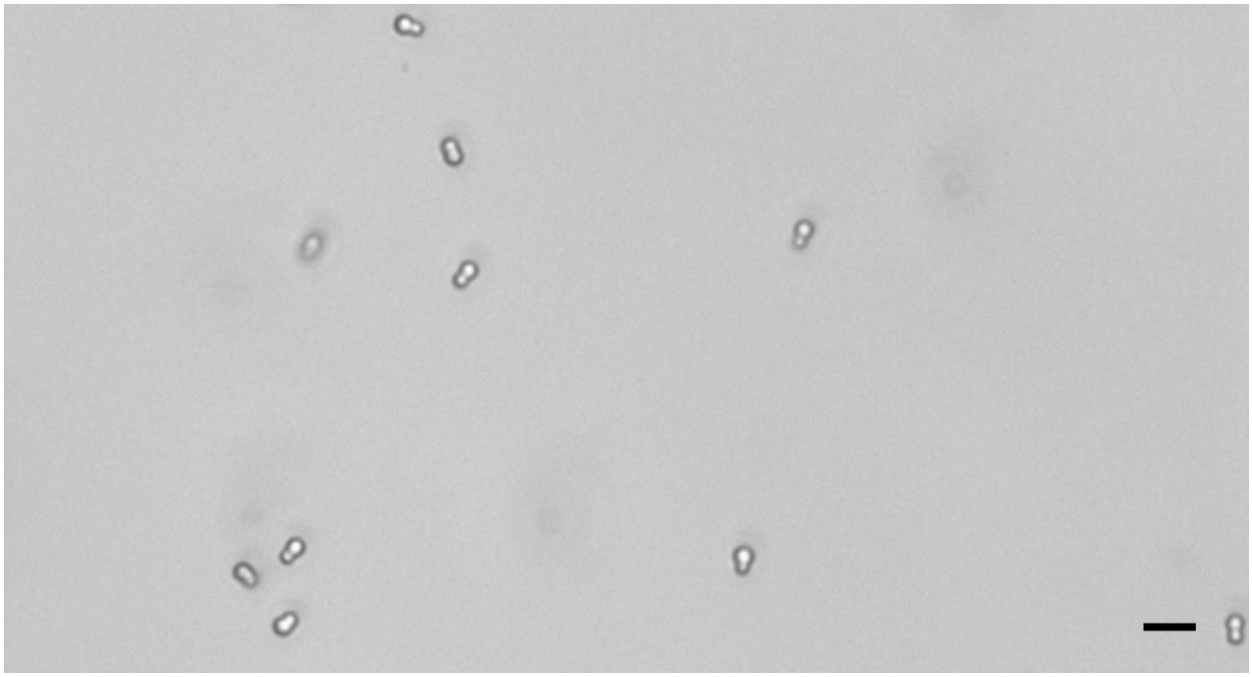

Figure 21 – swelling test with toluene (swelling ratio = 4) with LPS-TMSPA (swelling ratio = 0.5) sample. The image was taken after three days of swelling. A 60x objective was used. The scale bar represents 5 μm.

After systematically researching, the following optimized conditions were found: 0.5 wt/vol% NaSS, 1 wt/vol% AIBN, styrene (swelling ratio = 1.5) and toluene (swelling ratio = 2.5), swelling for 29 hours and polymerizing for 17 hours. The resulting particles can be seen in Figure 22 and Figure 23. When using a lower swelling ratio, no protrusions were formed.

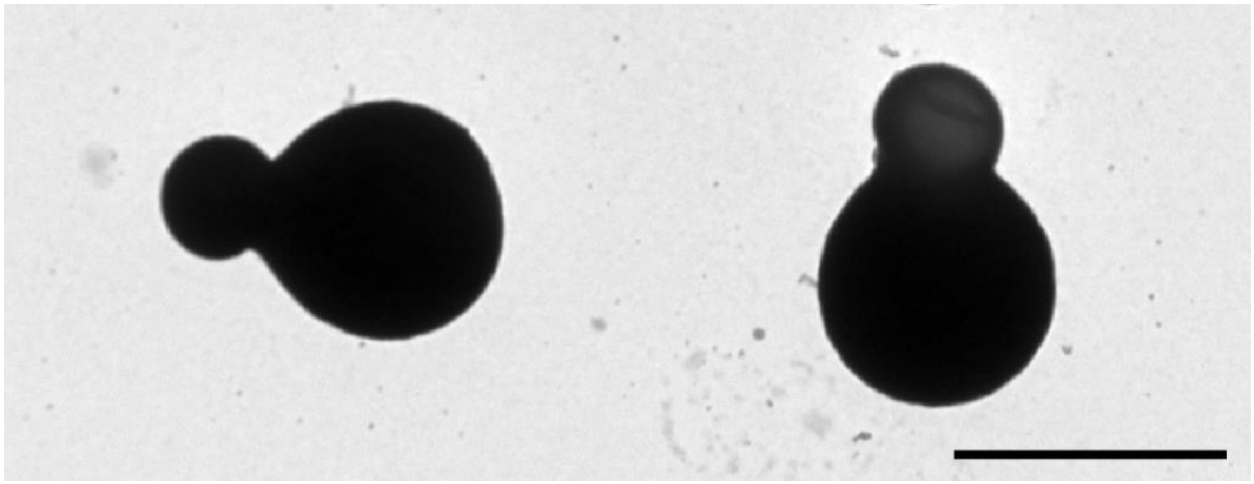

Figure 22 – TEM image of sample created using LPS-TMSPA (created using a swelling ratio of 0.5), styrene (swelling ratio = 1.5) and toluene (swelling ratio = 2.5). The scale bar represents 2 μm. The particle on the left is 2.55 μm long and its seed is 1.76 μm wide. The particle on the right is 2.56 μm long and 1.73 μm wide.

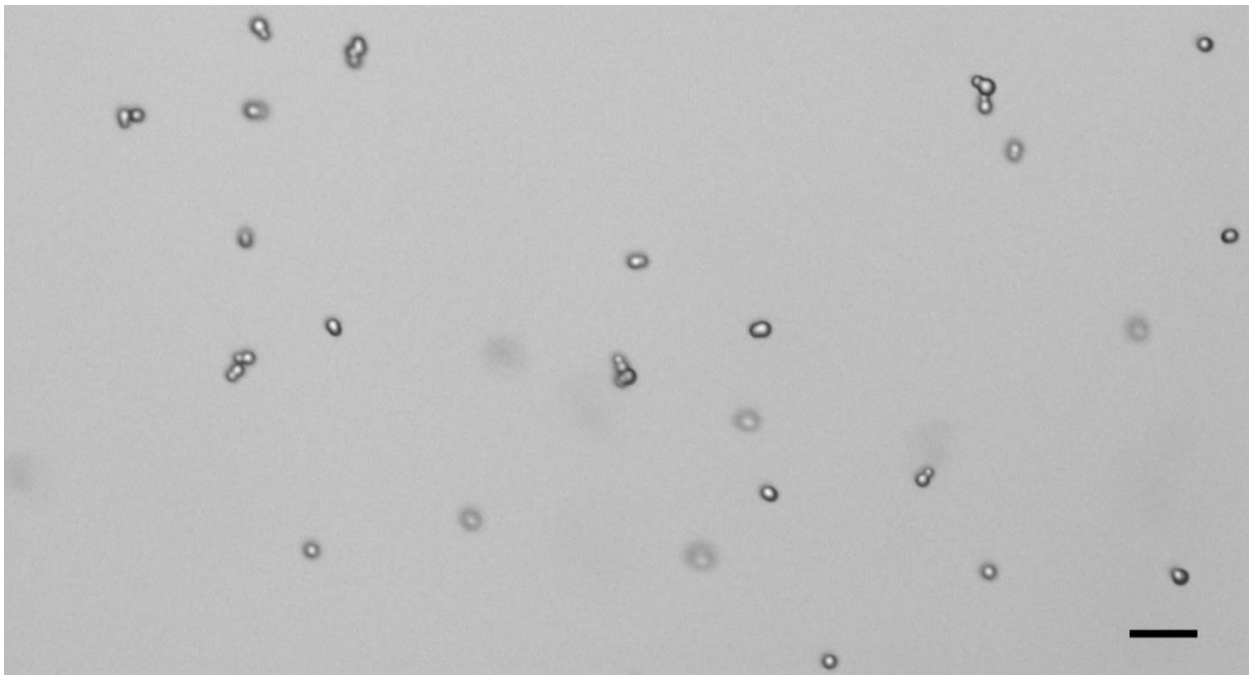

Figure 23 – image of the same particles as in Figure 22, but now in water. Image taken using optical microscopy (40x objective) directly after the polymerization reaction. The scale bar represents 10 μm.

The particles were modified using HMDS to be hydrophobic. The modified particles were laid out on an oil-water interface, see Figure 24. We see that aggregates are still formed immediately after injection. However, unlike what we saw for particles with a crosslinked shell (see Figure 16 and Figure 17),, the seed lobes of these particles do not attract each other. This means that the capillary interactions that were caused by the surface roughness have been largely eliminated. Now only the shape-induced capillary interactions remain.

In Figure 24 three dominant dimer structures are displayed, which seem to be the building blocks of the larger aggregates. As noted in the theory, the two structures displayed on the bottom left of Figure 24 are desired. The structure on the bottom right not desired. This structure should be higher in energy than the first two structures, but the structure still occurs frequently. There are also other, rarer dimer structures visible at the interface.

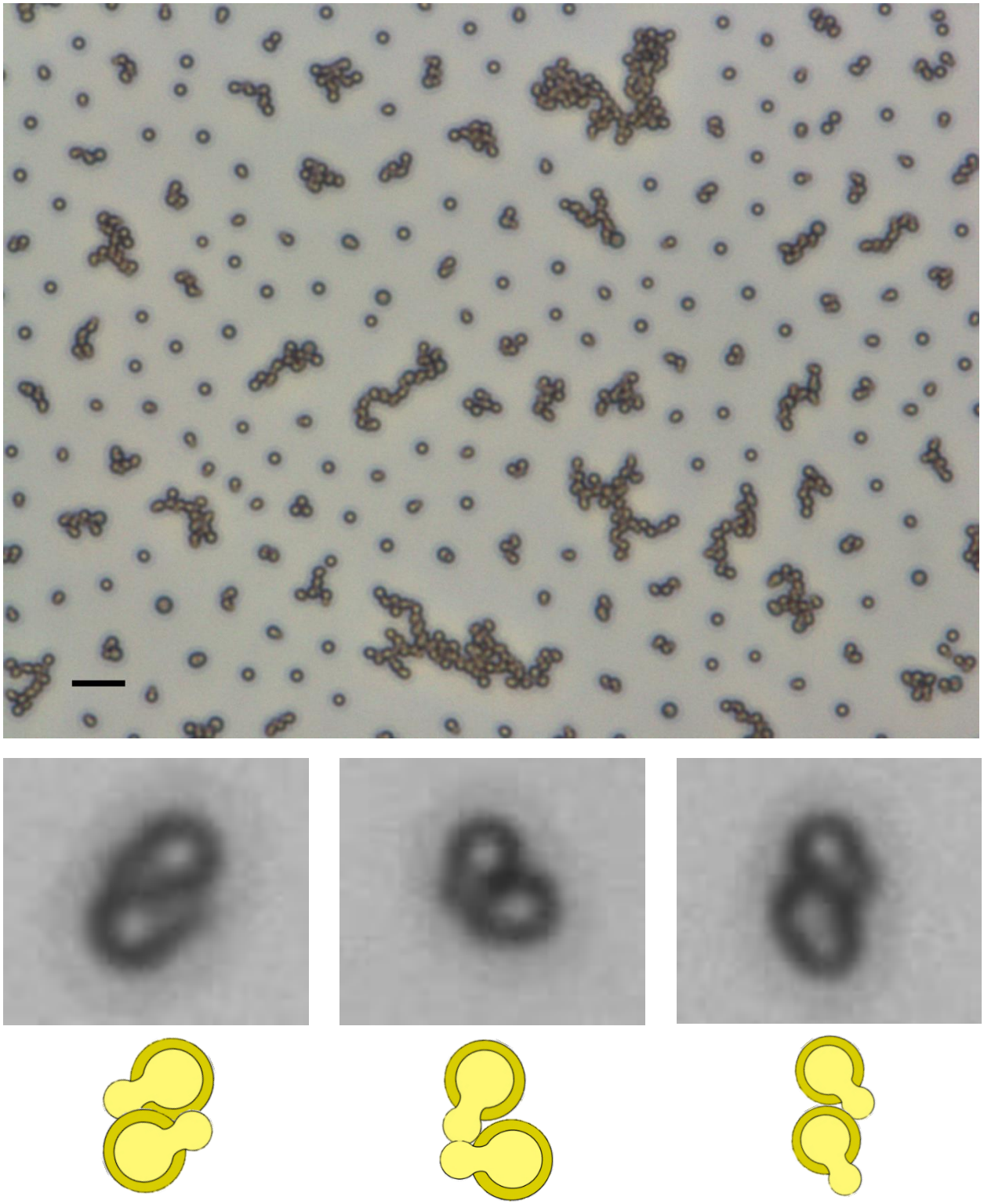

Figure 24 – particles at the oil-water interface. Top row: overview of interface, taken using optical microscopy (40x objective). The scale bar represents 10 μm. Center and bottom row: photos and drawings of three dominant dimer structures. The same particles as in Figure 23 are used, but the sample has now been modified using HMDS to be hydrophobic.

In another interface experiment using the same particles, the particles were tracked over time. See Figure 25. We can see the aggregates are getting larger and larger over time, and less and less monomers remain. Note that the monomers that remain in the third and fourth image in Figure 25 are

probably all spherical: these particles have no shape-induced capillary interactions, and therefore take a longer time before they become part of an aggregate.

The timescale of the formation of aggregates is quite short compared to other interface experiments by my supervisor. A reason could be that there is still toluene in the particles, which evaporates over the hours. This causes the particles to shrink, which causes surface roughness and capillary attractions.

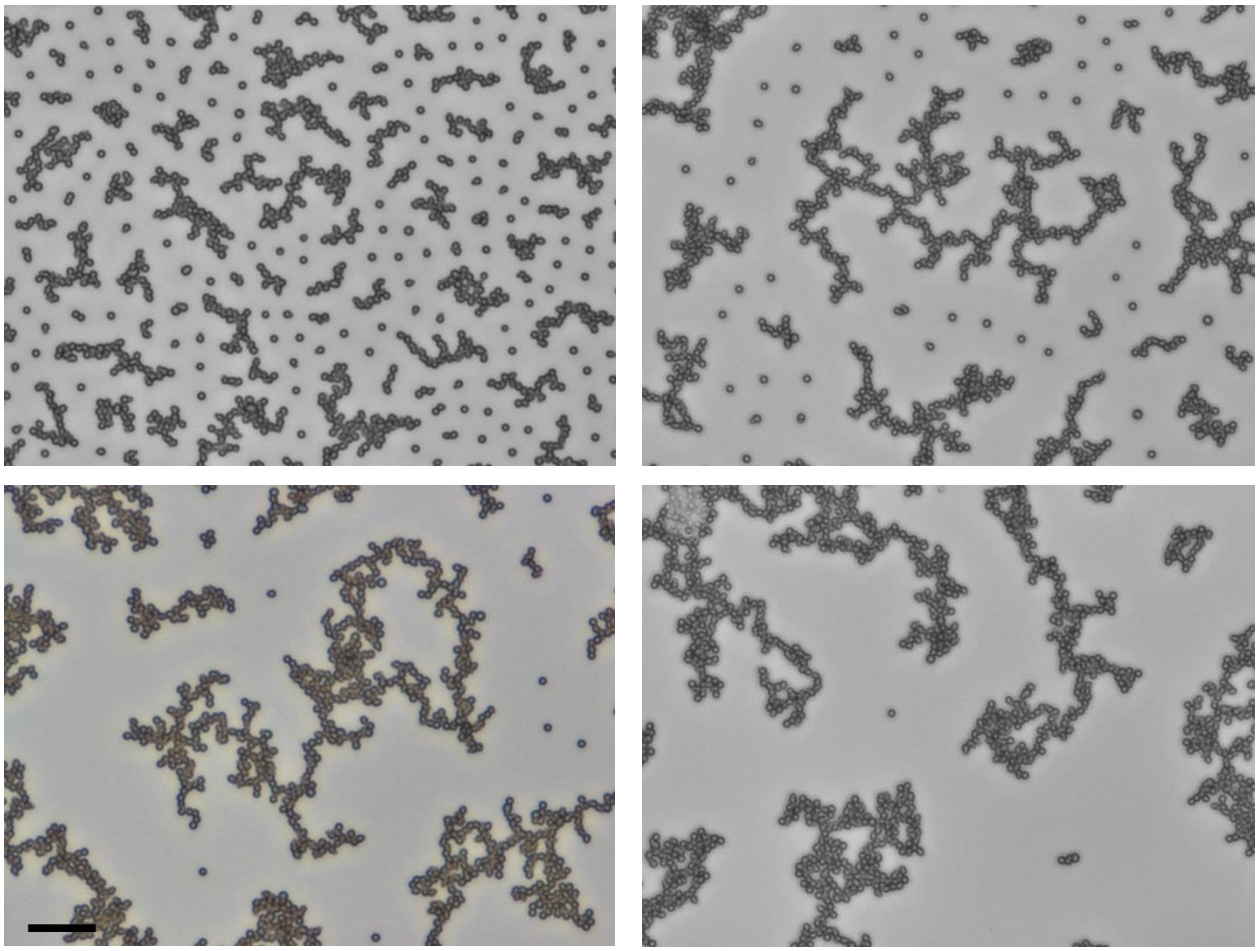

Figure 25 – evolution of interface system (decane-water) over time, using the same particles as in Figure 24. Time after injection, left to right, top to bottom: 0 hours, 2 hours, 4 hours, 6 hours. The images were taken using optical microscopy (40x objective). The scale bar represents 20 μm.

When using the same amounts, but using a newer bottle of styrene, swelling for 22 hours and polymerizing for 22.5 hours, the resulting protrusions were much smaller. This either means that the recipe is not very reproducible, that the recipe is very sensitive to the polymerization time or that the old bottle of styrene (which was a few years old) contained some impurities. TEM was used to take pictures of the sample. The particles can be seen in Figure 27, left. Based on 19 particles, the length of the particles is 1.99 ± 0.12 μm and the width is 1.75 ± 0.07 μm.

The last batch of particles that we synthesized were created using the following conditions: 0.5 wt/vol% NaSS, 1 wt/vol% AIBN, styrene (swelling ratio = 2, also using the newer bottle of styrene) and toluene (swelling ratio = 2), swelling for 27 hours and polymerizing for 19 hours. This batch is much more stable at the oil-water interface: a larger percentage of the particles is alone. See Figure 26.

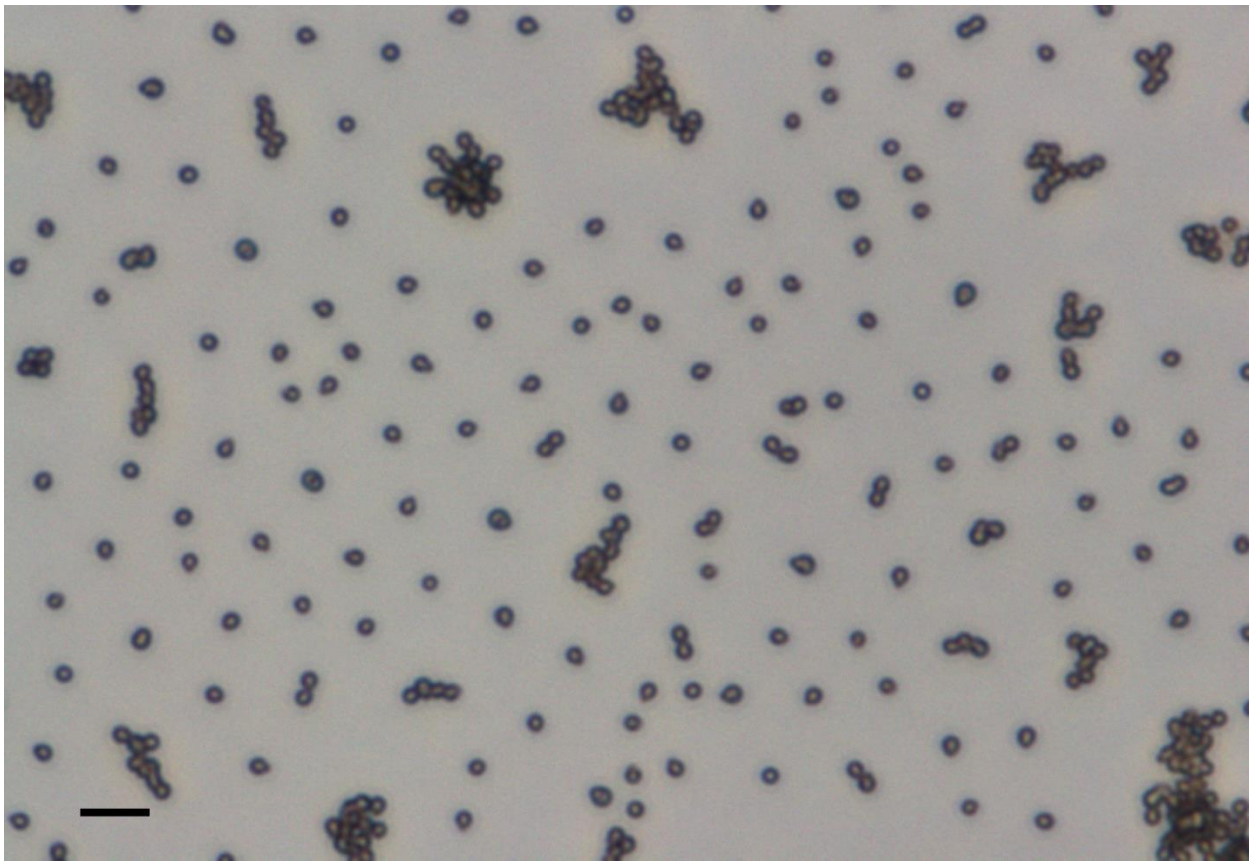

Figure 26 – Sample created using LPS-TMSPA (created using a swelling ratio of 0.5), styrene (swelling ratio= 2) and toluene (swelling ratio = 2) and modified using HMDS at the decane-water interface, The image was taken using optical microscopy (40x objective). The scale bar represents 20 μm.

Again, we used TEM to take a look at the particles (Figure 27, right). The particles had a length of 2.3 ± 0.3 μm and a width of 1.82 ± 0.17 μm. The particles are not very uniform in size and shape, the protrusion is sometimes smaller, somethings bigger. We can also see one particle where the protrusion is colored lighter – is this a hollow protrusion?

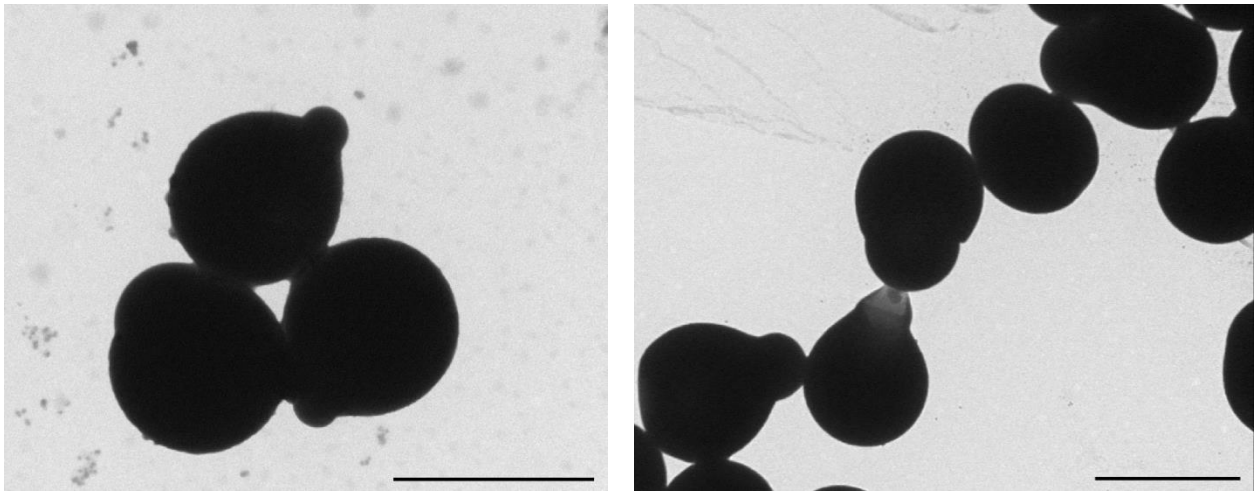

Figure 27 – TEM images of particles. Left: sample created using LPS-TMSPA (created using a swelling ratio of 0.5), styrene (swelling ratio = 1.5) and toluene (swelling ratio = 2.5). Although these amounts are the same as the amounts used for an earlier sample (Figure 23, Figure 24 and Figure 25), the particles have a smaller protrusion. Right: sample created using LPS-TMSPA (created using a swelling ratio of 0.5), styrene (swelling ratio= 2) and toluene (swelling ratio = 2). Both scale bars are 2 μm.

When using the same conditions, but using a longer polymerization time (27 hours), the particles tend to form aggregates. See Figure 28.

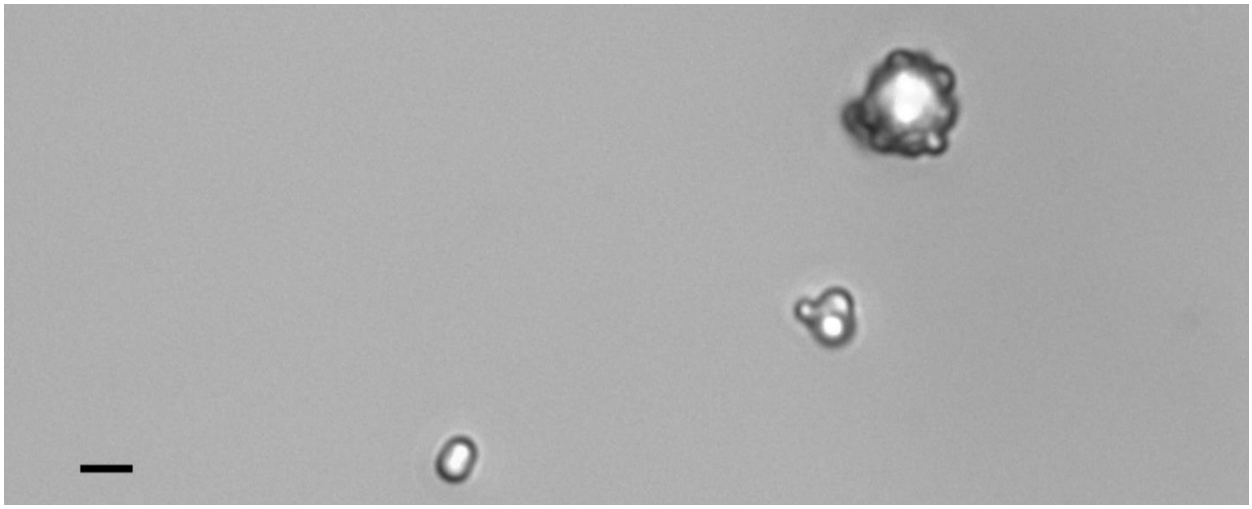

Figure 28 – sample created using the same conditions as in Figure 26, except that the polymerization time was much longer. This causes the particles to form small aggregates. Image taken of particles in water using optical microscope using a 60x objective. The image was taken after the polymerization step. The scale bar represents 5 μm.

5 Conclusions

Chemically anisotropic snowman-shaped particles were synthesized. Using fluorescence microscopy, we confirmed that the particles are indeed chemically anisotropic. Using transmission electron microscopy, we found out that the particles are not yet very homogenous in size, nor in shape.

The optimal conditions for synthesizing snowman-shaped particles depend on whether the core-shell particles contain DVB. When this is the case, synthesizing the particles requires a low swelling ratio (around 1.5). Otherwise, creating protrusions is more difficult, so a thinner shell, a higher swelling ratio (around 4) and a longer swelling time (around 28 hours) is required.

The particles are not yet very stable at the decane-water interface: the particles tend to aggregate both during injection and over time. Directly after injection the shape-induced capillary attraction seems to be the dominant interaction. This is promising for the future development of microstructures based on these particles.

The aggregation over time can probably be explained by the addition of toluene. Although toluene is useful for creating small protrusions, an unfortunate side effect is that the seed lobe of the particles can shrink over time. This results in a rough surface on the seed lobe, which enhances the capillary attractions and causes irreversible aggregation.

6 Outlook

The snowman-shaped particles offer potential for the formation of ordered structures. Until now, we have not been able to create such structures. We can try to make particles that are more uniform in size. We can also try to further reduce the amount of spheres in the sample. Both should offer improvement for the stability of the particles at the decane-water interface.

We do not know the contact angles of the particles at the interface yet. There are several methods to measure the contact angle. [21] One example of such a method is the gel-trapping method, which turns the water layer into a gel, allowing us to peel off the particles using a silicone elastomer. [21] We can then view the particles using scanning electron microscopy. If we know the contact angle, we can calculate the total surface free energy of the particles. [9]

The images of the interface are not very clear; we often cannot see where the protrusion on a particle is. Especially for smaller protrusions, it would be nice to have some way of highlighting the protrusions. As the protrusions is chemically inert, it will be very difficult to selectively attach a fluorescent dye.

An interesting experiment would be to let the snowman-shaped particles swell in toluene. If, as we expect, the protrusion takes up more toluene than the seed lobe, it will be possible to create dumbbell particles. From previous experiments by Fuqiang Chang, we know that it is then possible to form line-like structures with all protrusions on the same side. If we then let the toluene evaporate by heating, the lines should transform themselves into rings (Figure 29).

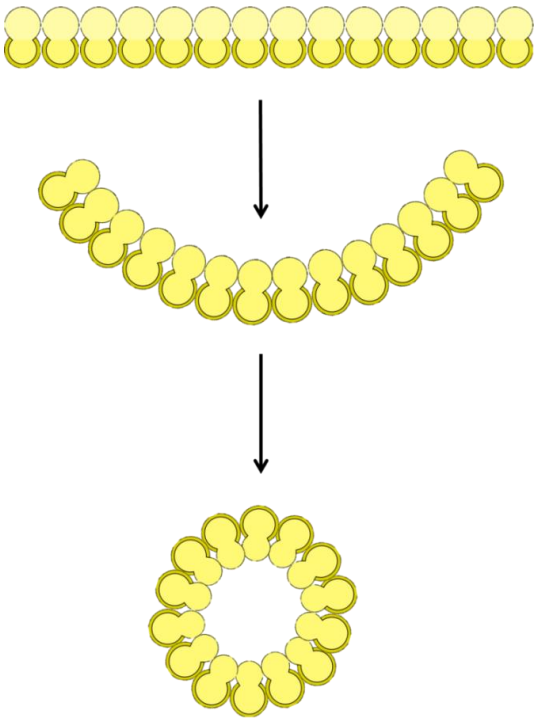

Figure 29 – first step: line of snowman-shaped particles swollen using toluene to dumbbell particles. Second and third step: when heating, the toluene will evaporate and the particles will get their original shape back. We hope that in doing so, the particles will form a ring.

Actually swelling the particles with toluene needs to happen in ethanol; if the reaction would be carried out in water, it will be difficult to transfer the particles to ethanol while preserving their shape. However, swelling in ethanol will be more difficult than swelling in water, as the toluene must be attracted to the particles in order to swell them.

7 Acknowledgements

I would like to thank my supervisor Fuqiang Chang, who taught me how to perform the laboratory work, and who always patiently answered any questions I had. I would also like to thank Yong Guo, Chris Evers and Samia Ouhajji for helping me with microscopy experiments. Finally, I would like to thank everyone at the Van het Hoff laboratory for the positive and friendly atmosphere.

Figure 30 – the Hugo R. Kruyt building. I worked in the wing on the right side of this image, on the seventh floor. Although the building is not the prettiest building in Utrecht, the layout of the building is very practical.

8 Bibliography

[1] G. M. Whitesides and M. Boncheva, "Beyond molecules: Self-assembly of mesoscopic and macroscopic components," *Proc. Nat. Acad. Sci.,* vol. 99, no. 8, pp. 4769-4774, 2002.

[2] D. H. Everett, Basic Principles of Colloid Science, Cambridge: Royal Society of Chemistry, 1994.

[3] B. J. Park and E. M. Furst, "Attractive interactions between colloids at the oil-water interface," *Soft Matter,* vol. 7, no. 17, p. 7676–7682, 2011.

[4] B. J. Park, C.-H. Choi, S.-M. Kang, K. E. Tettey, C.-S. Lee and D. Lee, "Geometrically and chemically anisotropic particles at an oil-water interface," *Soft Matter,* vol. 9, no. 12, pp. 3383-3388, 2013.

[5] B. P. Binks, "Particles as surfactans - similarities and differences," *Curr. Opin. Colloid Interface Sci.,* vol. 7, no. 1-2, pp. 21-41, 2002.

[6] B. Madivala, J. Fransaer and J. Vermant, "Self-Assembly and Rheology of Ellipsoidal Particles at Interfaces," *Langmuir,* vol. 25, no. 5, pp. 2718-2728, 2009.

[7] G. Fonnum, E. Weng, E. M. Aksnes, R. Nordal, P. C. Mørk, S. Tøgersen and J. Cockbain, "Process for the preparation of functionalized polymer particles". US Patent 6,984,702 B2, 10 June 2006.

[8] D. J. Kraft, W. S. Vlug, C. M. van Kats, A. van Blaaderen, A. Imhof and W. K. Kegel, "Self-Assembly of Colloids with Liquid Protrusions," *J. Am. Chem. Soc.,* vol. 131, no. 3, pp. 1182-1186, 2009.

[9] A. Kumar, B. J. Park, F. Tu and D. Lee, "Amphiphilic Janus particles at fluid interfaces," *Soft Matter,* vol. 9, no. 29, pp. 6604-6617, 2013.

[10] J.-G. Park, J. D. Forster and E. R. Dufresne, "High-Yield Synthesis of Monodisperse Dumbbell-Shaped Polymer Nanoparticles," *J. Am. Chem. Soc.,* vol. 132, no. 17, p. 5960–5961, 2010.

[11] J.-W. Kim, R. J. Larsen and D. A. Weitz, "Synthesis of Nonspherical Colloidal Particles with Anisotropic Properties," *J. Am. Chem. Soc.,* vol. 128, no. 44, pp. 14374-14377, 2006.

[12] T. S. Horozov, R. Aveyard, J. H. Clint and B. P. Binks, "Order-Disorder Transition in Monolayers of Modified Monodisperse Silica Particles at the Octane-Water Interface," *Langmuir,* vol. 19, no. 7, pp. 2822-2829, 2003.

[13] B. J. Park, J. P. Pantina, E. M. Furst, M. Oettel, S. Reynaert and J. Vermant, "Direct Measurements of the Effects of Salt and Surfactant on Interaction Forces between Colloidal Particles at Water-Oil Interfaces," *Langmuir,* vol. 24, no. 5, pp. 1686-1694, 2008.

[14] P. Pieranski, "Two-Dimensional Interfacial Colloidal Crystals," *Physical Review Letters,* vol. 45,

no. 7, pp. 569-572, 1980.

[15] D. Stanou, C. Duschl and D. Johannsmann, "Long-range attraction between colloidal spheres at the air-water interface: The consequence of an irregular meniscus," *Physical Review E,* vol. 62, no. 4, pp. 5263--5272, 2000.

[16] S. Reynaert, P. Moldenaers and J. Vermant, "Control over Coiloidal Aggregation in Monolayers of Latex Particles at the Oil - Water Interface," *Langmuir,* vol. 22, no. 11, pp. 4936-4945, 2006.

[17] J.-C. Loudet, J. Zhang, A. G. Yodh and A. M. Alsayed, "Capillary Interactions Between Anisotropic Colloidal Particles," *Physical Review Letters,* vol. 94, no. 1, p. 018301, 2005.

[18] B. G. P. van Ravensteijn, "Synthesis of Anisotropic Colloids from Chlorinated Seed Particles," in *Isotropic and Patchy Colloids with Engineerded Surface Functionality*, Utrecht, PhD Thesis, 2015, pp. 35-65.

[19] C. J. Brinker, "Hydrolysis and condensation of silicates: effects on structure," *Journal of Non-Crystalline Solids,* vol. 100, no. 1, pp. 31-50, 1988.

[20] C. A. Bruynes and T. K. Jurriens, "Catalysts for Silylations with 1,1,1,3,3,3-Hexamethyldisilazane," *J. Org. Chem.,* vol. 47, no. 20, pp. 3966-3969, 1981.

[21] V. N. Paunov, "Novel Method for Determining the Three-Phase Contact Angle of Colloid Particles Adsorbed at Air-Water and Oil-Water interfaces," *Langmuir,* vol. 19, no. 19, pp. 7970-7976, 2003.